Final Report for NEHRP Grant 06HQGR0031

Detecting hidden, high-slip rate faults: S. San Jacinto fault zone

Susanne U. Janecke PI

4505 Old Main Hill
Department of Geology
Utah State University
Logan UT 84322-4505

Report by Benjamin E. Belgarde and Susanne U. Janecke

2008

This final report is a prepublication manuscript by Belgarde and Janecke. It is also

Chapter 3 in Belgarde's MS thesis.

Publications from this research include one MS thesis, three abstracts, and one invited talk for the Second annual SoSAFE meeting in Pomona, California, Jan 31-Feb 2, 2008.

Belgarde, Benjamin, 2007, Structural characterization of the three southeast segments of the Clark fault, Salton Trough, California [M.S thesis]: Utah State University: 4 plates, map scale 1:24,000. 216 p. (Benjamin Belgarde's 2007 MS thesis consists of two prepublication manuscripts and three other thesis chapters)

INVITED TALK presented by Janecke:

Belgarde, B., and Janecke, S. U., 2007, A "hidden" fault? Structural geology of three segments of the Clark fault, San Jacinto fault zone, California: 20 minute presentation for SoSAFE workshop, Pomona California. Talk by Janecke and Belgarde will be posted in the near future.

ABSTRACTS:

Janecke, S. U., Belgarde, B. E., 2007, The width of dextral fault zones and shallow decollements of the San Jacinto fault zone, southern California: Annual meeting of the Southern California Earthquake Center, Palm Springs, CA, v. 17. http://www.scec.org/meetings/2007am/index.html

Cross-sectional, structural, geomorphic and map analysis of recently relocated earthquakes (Shearer et al., 2005) reveals steep NE dips and transpression across much of the San Jacinto fault zone in accord with growing evidence for widespread transpression across the southern San Andreas fault (Fuis et al., 2007). The seismically defined San Jacinto fault zone in the Peninsular Ranges is typically 9-10 km wide perpendicular to microseismic alignments, 12-15 km wide in map view, and consists of several identifiable steeply NE-dipping alignments of seismicity in the middle to lower seismogenic crust. The geologically defined fault zone is narrower in the same area. The width of the Clark fault zone in the Salton basin, on the other hand, is up to 13 km wider at the surface than the seismically active central part of the fault zone in the subsurface between 3 and 12 km depth (Belgarde, 2007). Mismatching shallow structures and deeper structures require flake tectonics and shallow decollements in some areas. These shallow decollements must have limited lateral extents because many parts of the adjacent fault zone persist as steep NE-dipping faults to 10-12 km depth from previously and newly mapped dextral faults at the surface. We correlate some NE-striking left-lateral faults with subsurface alignments of microseismicity; there are more right-lateral faults highlighted by microseismicity then left-lateral ones. A secondary concentration of earthquakes between 3-5 km depth may be the locus of decollements within the Salton basin or might be a zone of greater fluid pressures.

In some places there are excellent correlations between active surface structures and seismicity at depth. In other areas active fault zones produced no earthquakes in the last 25 years. We interpret those seismically quiet areas as locked or inactive during the period of study. Examples include many segments of the Coyote Creek fault, the Extra fault, the San Felipe Hills fault, and the northern third of the Clark fault zone in the Arroyo Salada segment. Another such area is a broad band along the SW margin of the Coachella Valley where numerous E and NE-facing fault scarps show Quaternary activity within a newly hypothesized fault zone that we here name the Torres Martinez fault zone. If further work confirms this fault zone it would have significant hazards implications because it projects northward to the most populated areas of the Coachella valley. We propose that deep Quaternary sedimentary basins SW of the dextral reverse parts of the San Jacinto and San Andreas fault zones are the result of the component of contraction across the strike-slip faults that likely dates back only 1-2 m.y., and are not as transtensional as previously thought. Deep Quaternary sedimentary basins SW of the dextral reverse parts of the San Jacinto and San Andreas fault zones are the result of the component of contraction across the strike-slip faults and are not as transtensional as previously thought.

Belgarde, B., and Janecke, S. U., 2007, A “hidden” fault? Structural geology of three segments of the Clark fault, San Jacinto fault zone, California: Geological Society of America Abstracts with Programs, Vol. 39, No. 6, p. 375.
http://gsa.confex.com/gsa/2007AM/finalprogram/abstract_129101.htm

We mapped and analyzed complexities of the Clark strand of the San Jacinto fault to better document its southeast extent and style of deformation. The Clark fault is a major fault with a lifetime slip rate of ~14.3± 0.7 mm/yr, yet its surface traces in the Salton Trough are poorly known. The fault's deformation zone widens southeastward from 1-2 km in the crystalline rocks of the Santa Rosa segment to ~ 18-km in the sedimentary rocks of the Salton Trough. The Clark fault continues ~ 25-30 km to the southeast of the termination point postulated by Dibblee (1954) and Sharp (1967), and 18 km beyond Sanders' (1989) Arroyo Salada segment, in agreement with Kirby et al. (2007). The Clark fault splays at the SE end of the Santa Rosa segment. The adjacent Arroyo Salada segment has abundant NW-striking scarps, is ~ 11-12 km long, and forms a complex web of faults and folds. A structural boundary at its southeast end consists of sinistral strike-slip faults that block the simple SE continuation of the fault zone. Southeast of the sinistral boundary we define the 12-13 km long San-Felipe-Hills structural segment with 4 subparallel deformation zones. Microseismicity broadens in plan view to the SE while narrowing with increasing depth from 12 km wide at 3 km depth to roughly 4±1 km wide below ~8 km depth. The Arroyo Salada segment contains two major NW-striking seismic alignments with a right-stepping geometry. Many alignments directly correlate to the central traces of the Clark fault zone. Other well-defined alignments do not correlate with the surface geology and require decollements within 5 km of the surface. Areas of few earthquakes suggest that the Truckhaven, San Felipe Hills, and West Calcite Mine Hill faults are seismically locked or inactive. NW-striking seismic alignments dip steeply towards the northeast whereas surface exposures of dextral faults dip southwest,

subparallel to bedding along flats in the faults. We infer a dip reversal along these faults roughly at the basement-cover contact (< 3 km). Better documentation of faults, folds, scarps, microseismicity and surface deformation in the San Jacinto zone provides insights into diffuse deformation within mud-rich sedimentary basins, and illustrates how the high seismic potential and hazard of such fault zones may be "hidden" from conventional methods of analysis.

Belgarde B. and Janecke, S. U., 2006, Structural Characterization and Microseismicity near the SE end of the Clark fault of the San Jacinto fault zone in the SW Salton Trough: Annual meeting of the Southern California Earthquake Center, Palm Springs, CA, v. 16, p. 75. http://www.scec.org/meetings/2006am/

Geological mapping in the eastern Borrego Badlands and the northwestern San Felipe Hills at a scale of 1:24,000 better characterizes the structural deformation near the SE end of the Clark fault. The Clark fault is one of the major NW-SE striking strike-slip faults of the San Jacinto fault zone. An abrupt change in the complexity and width of the surface trace of the Clark fault occurs as it enters the San Felipe-Borrego basin from the NW. The structural deformation observed within the sedimentary rocks is much more complex than in the crystalline rocks to the NW. Fold trains, fault bends, left-lateral and normal connecting faults and stopovers connect short dextral faults, and locally NE-striking left-lateral faults cut across much of the fault zone in the San Felipe-Borrego basin. Microseismicity along the Clark fault zone mirrors the structural deformation. Near the southeastern end of the Santa Rosa segment a ~2 km wide zone of small earthquakes coincides with the surface trace of the Clark fault, yet to the SE in the San Felipe Hills segment the seismic zone widens to at least ~12 km. The Arroyo Salada segment has a broad zone of distributed faults that merge with a central zone of parallel faults and scarps directly along strike of the Clark fault in the Santa Rosa segment and define a main fault zone about 2 km wide with up to 7 separate fault strands. Fault scarps with mostly SW-down dip-slip displacement cut middle Pleistocene to Holocene pediment gravels. Splays north of this main zone curve northward and connect to a series of N-S striking normal faults with dominantly east-side down displacements. Some of the normal faults offset Pleistocene pediment gravels. The main fault zone in the Arroyo Salada segment cuts the common SSW-dipping limb between the large NW-plunging Borrego syncline in the southwest and the W-trending Grave's Wash anticline in the north, and thus occupies an intermediate structural position. We define a San Felipe Hills segment of the Clark fault that persists at least 14 km farther to the SE. It is characterized by a broad zone of a radiating dextral faults and closely-spaced detachment folds, which coincides with a NW-trending structural high. The largest structure in the San Felipe Hills area is the NW-SE striking dextral strike-slip Dump fault. Recent microseismicity along the Dump fault has produced multiple small earthquakes with magnitudes of up to 4.3 and confirms that this is the main structure in the fault zone. The maximum right-separation along this fault is ~4-5 km, which leaves ~10 km of a near surface slip deficit since the sedimentary rocks were tilted. Despite this large near-surface slip deficit it is clear

STRUCTURAL CHARACTERIZATION OF THREE SOUTHEAST SEGMENTS OF THE CLARK FAULT, SALTON TROUGH CALIFORNIA

by

Benjamin E. Belgarde

A thesis submitted in partial fulfillment
of the requirements for the degree

of

MASTER OF SCIENCE

in

Geology

Approved:

_____	_____
Dr. Susanne U. Janecke	Dr. James P. Evans
Major Professor	Committee Member
_____	_____
Dr. John W. Shervais	Dr. Byron R. Burnham
Committee Member	Dean of Graduate Studies

UTAH STATE UNIVERSITY
Logan, Utah

2007

ABSTRACT

Structural Characterization of Three Southeast Segments of the Clark Fault, Salton Trough California

by

Benjamin E. Belgarde, Master of Science

Utah State University, 2007

Major Professor: Dr. Susanne U. Janecke
Department: Geology

We examine the structural complexities of a 28-km long part of the Clark fault of the San Jacinto fault zone in southern California in order to better document its lateral extent and the style of deformation of its southeast end. Changes in structural style are observed as the Clark fault's damage zone widens from ~ 1-2 km in crystalline rocks of the Peninsular Ranges southeastward to ~ 18 km in the sedimentary rocks of the San Felipe-Borrego subbasin of the Salton Trough. The Clark fault extends into the San Felipe-Borrego subbasin as the Arroyo Salada segment for ~ 11-12 km to a newly defined northeast-trending structural boundary. This structural boundary, referred to herein as the Pumpkin Crossing block, is a ~ 3-km wide and ~ 8-km long fault zone dominated by northeast-striking sinistral-normal strike-slip faults. Southeast of the Pumpkin Crossing block the newly defined San Felipe Hills segment extends the Clark fault another ~12-13 km southeast to its intersection with the Extra fault zone. The Clark fault may have nearly 14.5-18 km of right separation represented in the surface

deformation of the Arroyo Salada and San Felipe Hills segments, but the total amount of strain is masked by the wide diffuse fault zone with its complex deformation patterns and geometries. The lateral change observed in microseismicity patterns across the Arroyo Salada and San Felipe Hills segment boundary supports our structural interpretations about the existence, location, and structure of this boundary. Vertical patterns in the microseismicity suggest that the Clark fault zone narrows at depth, dips steeply northeast in the subsurface, and must interact with at least one weak decollement layer(s) beneath and/or with the sedimentary basin.

Structural deformation within the late Miocene to Holocene silty- and clay-rich sedimentary basin of the Salton Trough includes features characteristic of strike-slip faults, such as stepovers, conjugate faults, folds, flower structures, and fault bends, as well as many unique structures that include pooch structures, ramp-flat geometries of strike-slip faults, complex en echelon fault zones with localized shear distributed across a high frequency network of faults, and heterogeneous kinematic indicators within individual fault zones.

(216 pages)

CONTENTS

Table Page

LIST OF FIGURES

CHAPTER 3

STRUCTURAL GEOLOGY OF THE THREE SOUTHEAST SEGMENTS OF THE CLARK FAULT, SALTON TROUGH, CALIFORNIA: IMPLICATIONS TO HAZARDS, SLIP RATES, AND SLIP AMOUNTS [1]

Abstract

Individual faults within the San Jacinto fault zone are structurally complex zones of deformation. We have examined the structural complexities along one of the strands of the San Jacinto fault, the Clark fault, in order to better document the southeast extent and style of deformation caused by this fault. Changes in structural style are documented along strike as the Clark fault's deformation zone widens southward from 1-2 km in the crystalline rocks of the Peninsular Ranges to ~ 18-km wide in the sedimentary rocks of the Salton Trough. This investigation studied the central 12 km of the Clark fault where it actively deforms the sedimentary rocks of the San Felipe-Borrego subbasin.

This study shows that the Clark fault continues ~ 25-30 km to the southeast of the termination point postulated by Dibblee (1954), Sharp (1967,1972), and Jennings (1977) and 18 km beyond Sanders' (1989) Arroyo Salada segment. The Arroyo Salada segment has abundant surface faulting and is ~ 11-12 km long zone. This segment is as wide as ~18 km and incorporates a complex deformation zone between the Truckhaven fault to the north and the San Felipe Hills fault to the southwest. A structural boundary at the southeast end of this segment called the Pumpkin Crossing block consists of multiple sinistral strike-slip faults that cut across the central traces of the Arroyo Salada segment. Beyond this structural boundary to the southeast we define an additional 12-13 km long

San Felipe Hills structural segment (Kirby, 2005; this study). This segment links deformation related to the Clark fault through the northern San Felipe- Borrego subbasin as far southeast as the crossing Extra fault zone. Geological mapping and structural analysis have characterized each of these segments in detail.

Interpretations of the microseismicity along the southeast portion of the Clark fault have further enhanced our structural investigation. Southeastward broadening zones of seismicity contain alignments that directly correlate to the central traces of the Clark fault in the Arroyo Salada segment. The seismic alignments dip steeply towards the northeast whereas surface exposures have southwest-dipping fault planes parallel to bedding. The microseismicity indicates a contractional reverse component because of northeast-side-up motion whereas the southwest-dipping surfaces indicate an extensional component. We link the surface deformation to seismic alignments and conclude that there is a dip reversal in the faults as they enter into the sedimentary rocks in the shallow crust (< 3 km). Surface traces of faults in the Pumpkin Crossing block also correlate with microseismic alignments, which indicate that this major fault zone of sinistral faults may also serve as a seismic boundary. Microseismic shadow zones or areas of few earthquakes around the San Felipe Hills fault and the Graves Wash fault suggest that these areas are seismically locked or inactive.

1. Introduction

The San Jacinto fault zone is a part of the San Andreas fault system and it is actively deforming the sedimentary rocks of the Salton Trough. The San Jacinto fault zone branches westward off of the San Andreas fault zone northwest of San Bernardino

and continues southeast as a series of strike-slip faults crossing through the meta sedimentary and plutonic rocks of the Peninsular Ranges as well as the sedimentary rocks of the Salton Trough (Dibblee, 1954; Sharp, 1967; Matti and Morton, 1993; Morton and Matti, 1993; Lutz et al., 2006; Kirby et al., 2007). The ~ 300-km long San Jacinto fault zone initiated between ~1.4 and 1.1 Ma as a response to an abrupt change in the plate boundary (Morton and Matti, 1993; Kirby, 2005; Janecke et al., 2006; Lutz et al., 2006; Kirby et al., 2007) (Fig. 3-1). Between 19 and 29 km of right separation (Sharp, 1967; Bartholomew, 1970; Hill, 1984; Matti and Morton, 1993; Janecke et al., 2005) is accommodated by a series of dextral strike-slip faults that generally trend ~130° (Dibblee, 1954; Sharp, 1967, 1975; Sanders, 1989). The southernmost faults of the San Jacinto fault zone in the Salton Trough region are the Coyote Creek, Superstition Hills, Wienert, Superstition Mountain and the Clark faults (Fig. 3-1). Structural and microseismic characteristics of the southeast part of the Clark fault are described and interpreted in this paper to improve our understanding of actively deforming fault zones in a transpressional tectonic setting.

The ~ 120 km long Clark fault's northern end begins near Hemet, California south of the Casa Loma fault (Sharp, 1967; Sanders, 1989) (Fig. 3-1). Approximately 24-25 km of right separation has been calculated along the Clark fault in the Anza segment to the northwest of the study area (Sharp, 1967). As major branches peel off the Clark fault towards the southeast the separation decreases to ~ 14.5 -18 km of right separation by the Santa Rosa segment (Sharp, 1967; Janecke et al., 2005). The simpler linear trace of the Clark fault through the Peninsular Range changes into a wide complex zone of deformation in the San Felipe-Borrego subbasin (Fig. 3-2). The Clark fault initiated in

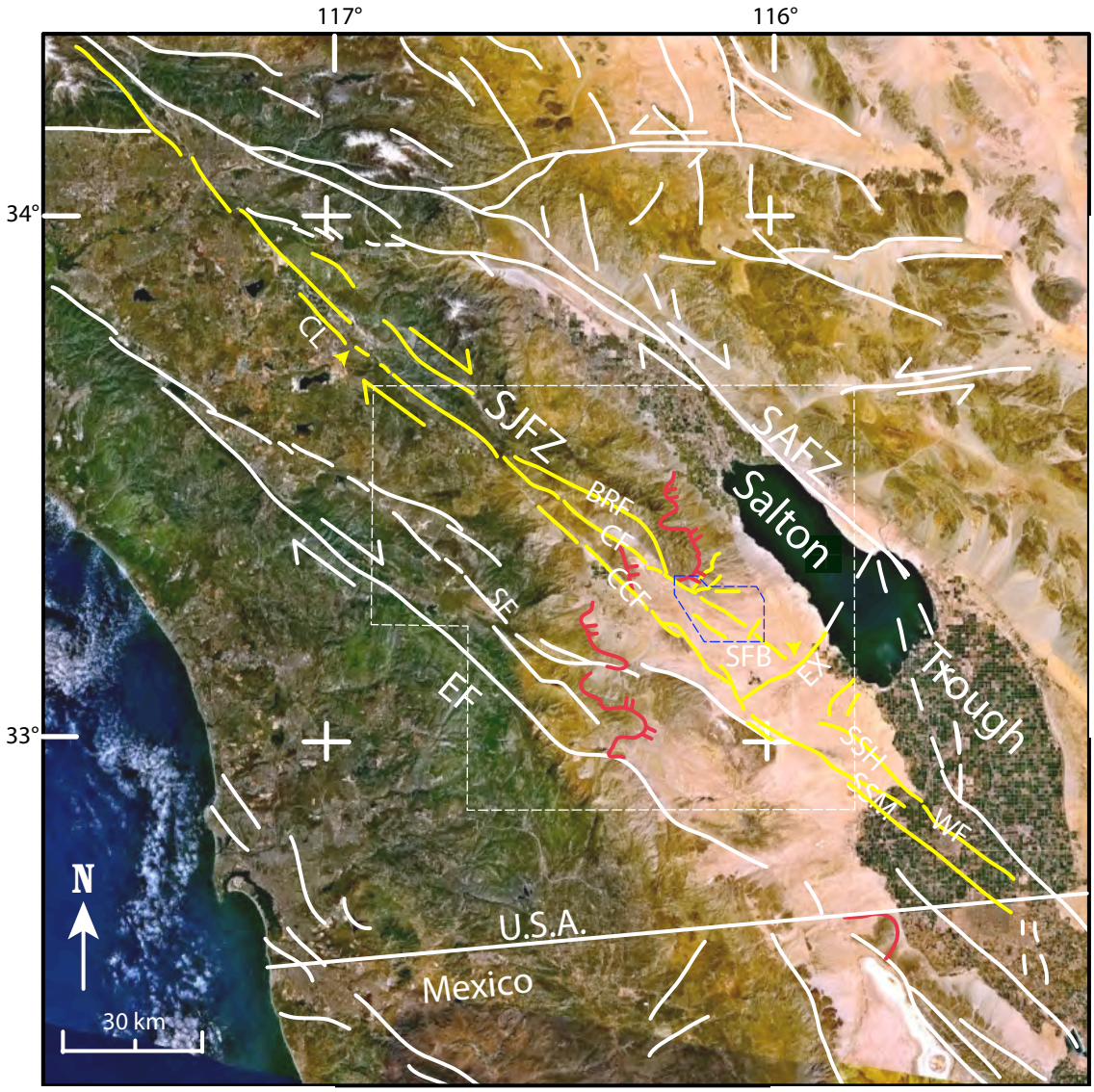

Fig. 3-1. NASA Learning Technologies Landsat 7 image of southern California showing major fault traces. White dashed line is the outline of figure 3-2 Blue dashed outline is the study area. Yellow lines are the major faults associated with the San Jacinto fault zone (SJFZ). Yellow arrows show beginning and end of the Clark fault. Red line is the West Salton detachment fault bars are on the hanging wall. BRF- Buck Ridge fault; CL- Casa Loma fault; CF-Clark fault; CCF- Coyote Creek fault; EF- Elsenore fault; EX- Extra fault zone; SAFZ- San Andreas fault zone; SF- San Felipe fault zone; SFB - San Felipe-Borrego subbasin; SSM- Superstitions Mountain fault; SSH- Superstition Hills fault; WF - Wienert fault. Fault locations compiled from Jennings (1977), Sanders (1989), and Magistrale (2002).

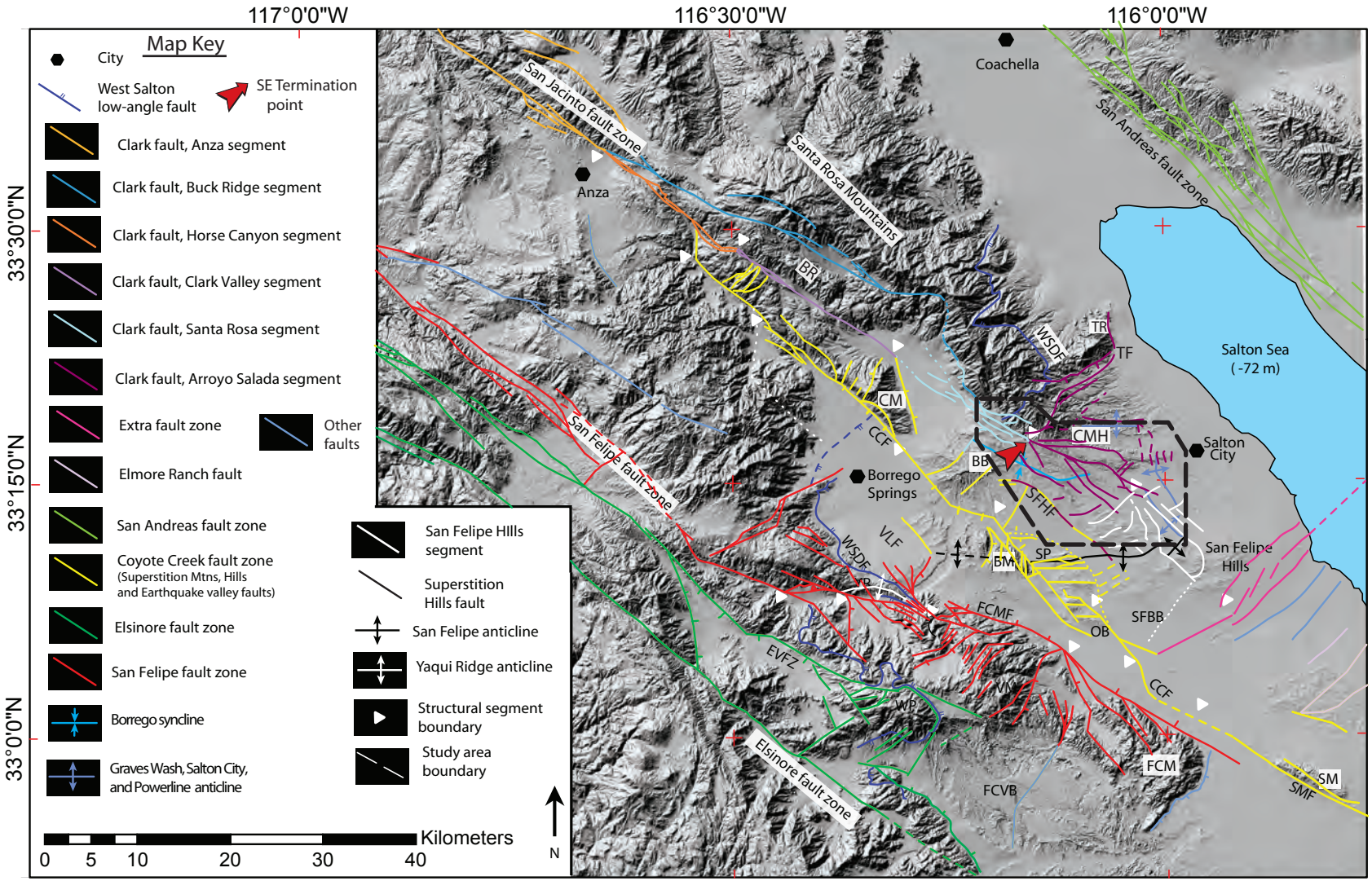
117°0'0"W
116°30'0"W
116°0'0"W
33°30'0"N
33°15'0"N
33°0'0"N
Map Key
City
West Salton low-angle fault
SE Termination point
Clark fault, Anza segment
Clark fault, Buck Ridge segment
Clark fault, Horse Canyon segment
Clark fault, Clark Valley segment
Clark fault, Santa Rosa segment
Clark fault, Arroyo Salada segment
Extra fault zone
Other faults
Elmore Ranch fault
San Andreas fault zone
Coyote Creek fault zone (Superstition Mtns, Hills and Earthquake valley faults)
Elsinore fault zone
San Felipe fault zone
Borrego syncline
Graves Wash, Salton City, and Powerline anticline
San Felipe HIlls segment
Superstition Hills fault
San Felipe anticline
Yaqui Ridge anticline
Structural segment boundary
Study area boundary
Kilometers
0 5 10 20 30 40
N
Coachella
San Jacinto fault zone
Anza
Santa Rosa Mountains
San Andreas fault zone
BR
WSDF
TR
TF
Salton Sea (-72 m)
CM
CCF
CMH
Salton City
San Felipe fault zone
Borrego Springs
BB
SFHF
VLF
BM
SP
San Felipe Hills
YR
FCMF
SFBB
OB
EVFZ
VM
WP
CCF
Elsinore fault zone
FCM
SM
FCVB
SMF

Fig. 3-2.

Fig. 3-2. Important active faults of southern California overlain on a shaded relief map. The study area is indicated by the black dashed lines. Segments along the Clark fault are color coded. BB-Borrego Badlands; BM-Borrego Mountain; BR- Buck Ridge; BRF-Buck Ridge fault; CCF-Coyote Creek fault; CF-Clark fault; EVFZ-Earthquake Valley fault zone; FCM-Fish Creek Mountains; FCMF-Fish Creek Mountains fault; FCVB - Fish Creek-Vallecito basin; OB-Ocotillo Badlands; SFHF- San Felipe Hills fault; SM-Superstition Mountain; TF-Truckhaven fault; TR-Travertine Ridge; VM-Vallecito Mountains; WSDF-West Salton detachment fault; YR-Yaqui Ridge. Faults and segments are compiled and modified from Rogers, 1965; Jennings, 1977; Sanders, 1989; Kennedy and Morton, 2003; Kirby, 2005; Lutz, 2005; Steely et al., submitted 2007; and this study.

this subbasin between ~ 1.0 - 1.1 Ma (Kirby, 2005; Lutz, 2005; Lutz et al., 2006; Kirby et al., 2007).

Geological mapping by Dibblee (1954, 1984), Hoover (1965), Sharp (1965, 1967, 1972), and Jennings (1977) identified the southeastern end of the Clark fault in the northern San Felipe- Borrego subbasin west of Smoke Tree Canyon based on the absence of a major fault zone farther to the southeast (Fig. 3-2). Since then many detailed studies have taken place to the southeast of this initial termination point, but none fully documented the deformation within the northern San Felipe-Borrego subbasin (Eckis, 1930; Bartholomew, 1968; Weismeyer, 1968; Reitz, 1977; Droynk, 1977; Feragen, 1986; Wesnousky, 1988; Wells, 1987; Pettinga, 1991, and unpublished mapping; Sanders and Magistrale, 1997; Ryter, 2002; Heitman, 2002; Lilly, 2003; Lutz, 2005; Kirby, 2005). A possible continuation past this end point was postulated by Sanders (1989) as a 12-km long zone of disconnected faults called the Arroyo Salada segment. Another more recent study documented ~ 5.62 ± 0.4 km of shortening and strike-slip deformation related to the Clark fault in the southeast and central San Felipe Hills ~ 18 km beyond Sanders' (1989) end point, but without the detailed investigation of the intervening segments it was impossible to verify the connection to the Clark fault (Kirby, 2005; Kirby et al., 2007). Our structural investigation has complied previous mapping with new 1:24,000 scale geological and structural mapping to examine the southeastern termination point of the Clark fault.

Although the major structural aspects of the San Jacinto fault zone have been well documented many structural relationships among and along individual faults remain incompletely understood. Previous analysis has revealed discontinuities within the San

Jacinto fault zone and approximately 20 individual segments have been identified (Dibblee, 1954; Sharp, 1967, 1972, 1975; Clark, 1972; Matti et al., 1985; Wesnousky, 1988, 1989; Sanders, 1989; Sanders and Magistrale, 1997). Segment boundaries along the San Jacinto fault zone have been identified using combinations of structural and seismic criteria. The Clark fault has previously been divided into seven major segments. Our structural investigation of the southeasternmost segments and the area to the southeast refines these segmentation models along the southeast part of the Clark fault. In this analysis we focus our attention first on the structural characteristics of the Clark fault and second on the correlation between mappable features and seismic signals.

Many geological models of strike-slip fault zones such as the wrench fault model and the strain partitioning model help explain the structures and their kinematic and geometric relationships to a given stress field (Fitch, 1972; Wilcox et al., 1973; Withjack and Jamison, 1986) (Fig. 3-3). These structural models have built on basic Andersonian theory to help explain complexities of strike-slip fault zones (Anderson, 1951; Wilcox et al., 1973; Withjack and Jamison, 1986) but they tend to be over simplified and do not adequately explain a large portion of the structures interpreted within this study area.

The Coyote Creek, Buck Ridge, Extra and West Salton detachment faults are the major structures in the region that may be affecting the strain of the Clark fault zone. The understanding of these major faults is just as crucial as the Clark fault as we interpret the linkages of structures beyond this fault zone in an attempt to better understand the regional strain field of the San Jacinto fault zone.

The Coyote Creek fault is the second largest dextral strike-slip fault within the San Jacinto fault zone at the latitude of this study. This fault diverges from the Clark

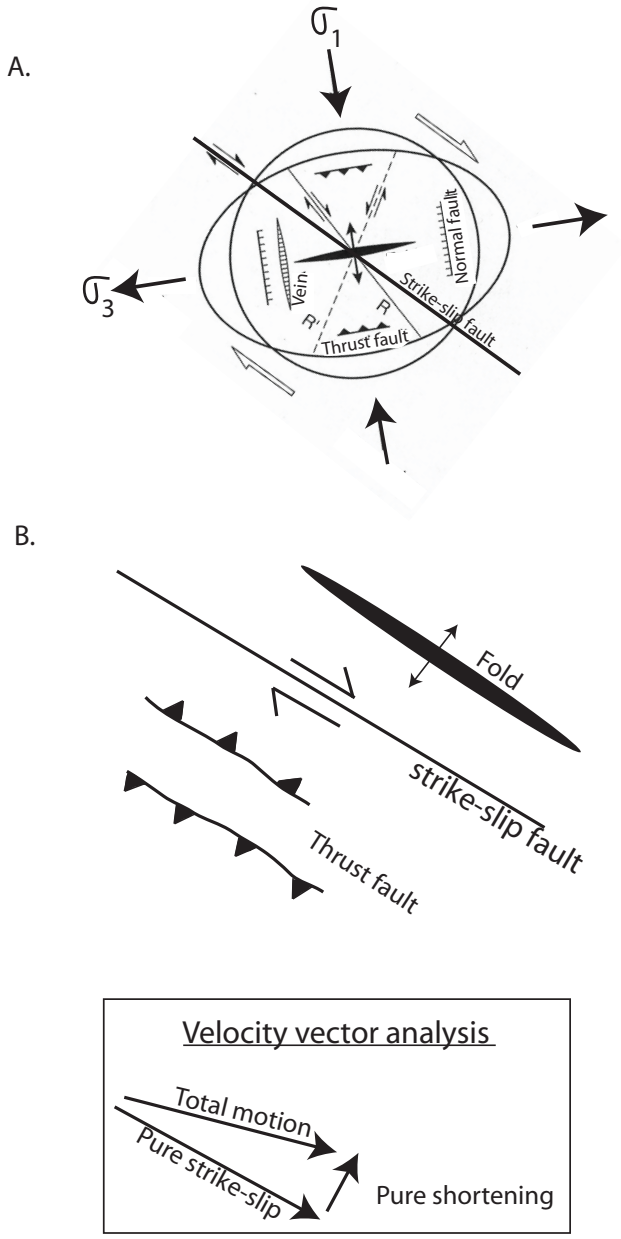

Fig. 3-3. Kinematic models of strike slip fault zones. (A) Wrench fault tectonics model modified from Van de Pluijm and Marshak, (2004) Detail of the strain ellipse showing that folds and thrusts form perpendicular to the shortening direction, while normal faults and veins form perpendicular to the extension direction. En echelon faults form parallel to sinistral and dextral strike-slip fault equivalent to R and R' shears. Direction of maximum horizontal stress (Sigma 1) was oriented north-northwest similar to the stress field associated with the Clark fault zone (Savage et al., 1974; Townend and Zoback, 2004). (B) Strain partitioning model. Map view showing a strike-slip fault oriented subparallel to thrusts and folds. Velocity vector analysis of total motion would predict the structures in the above figure. Total motion is subdivided into pure shortening and pure strike-slip components (Fitch, 1972).

fault ~ 5 km to the southwest as a zone of interconnected fault stepovers and bends for ~ 80-90 km until linking up with the Superstition Mountain fault in the southeast (Fig. 3-2). The Coyote Creek fault accounts for ~1.0 - 4.8 km of right separation (Sharp, 1967; Janecke et al., 2005). The Buck Ridge fault is another major fault that branches off the Clark fault zone eastward near the northern end of the Horse Canyon segment of the Clark fault (Fig. 3-2). The western two thirds of the Buck Ridge fault strikes ~120° and diverges from the Clark fault (Dibblee, 1954; Sharp, 1967; Sanders, 1989). The fault cuts through the Santa Rosa Mountains northeast of the Horse Canyon, Clark Valley, and Santa Rosa segments of the Clark fault (Fig. 3-2). Previous mapping has poorly documented the southern extent of this fault (Dibblee, 1954; Sharp, 1967; Sanders, 1989).

The West Salton detachment fault is a low-angle normal fault that is offset by the Clark fault. A part of this fault is located east of Palo Verde Canyon in the northwest part of the study area and forms the basin margin between the crystalline rocks and the late Cenozoic sedimentary rocks. The detachment fault dips ~ 12-20 ° and projects under most of the northern part of study area (Plate 3, A-A', B-B'). The detachment fault is not exposed on the southwestern side of the Clark fault, but we suspect that it is covered by Quaternary alluvium west of Coyote Mountain.

The Extra fault zone is a series of en echelon right-stepping sinistral strike-slip faults that are connected to both the San Jacinto fault zone and the San Andreas fault zone (Hudnut et al., 1989; Janecke, unpublished mapping). This series of discontinuous northeast-southwest trending sinistral faults cross and ultimately terminate the Clark fault in the southeast San Felipe Hills (Hudnut et al., 1989; Janecke, unpublished data).

Interaction of these conjugate faults produced the highly deformed San Felipe Hills (Kirby, 2005).

The Clark fault is the source of hundreds of small earthquakes every year (Thatcher et al., 1975; Sanders, 1989; SCSN database). These earthquakes provide additional information about the subsurface structure of the fault zone, its rupture segmentation, its lateral and depth extent, its rheology and its strain patterns. Earthquakes with magnitudes up to 4.2 M_L persist more than 20 km southeast of the traditional endpoint of the fault and form a southeast widening wedge in map view. This seismic zone was used to lengthen the Clark fault 12km to the southeast of the previous end point due to the aftershocks of the M_w 6.4 Arroyo Salada earthquake (Sanders, 1989).

Precise relocation of these earthquakes using various cluster analysis, cross correlations and double-difference methods are available, but few of the relocated data have been analyzed along this part of the San Jacinto fault, nor have possible correlations between surface structures and active structures at depth been examined (Richards-Dinger and Shearer, 2000; Hauksson et al., 2004; Hauksson and Shearer, 2005; Shearer et al., 2005). A southwest-dipping Clark fault inverted from Hauksson's (2000) relocated earthquake catalog using Gocad 3D modeling software (Suppe, 2003), suggests an extensional component across the southeast end of the Clark fault because the vertical sense of slip across the fault inferred from the fault scarps is mostly southwest-down (Sharp, 1967,1972; this study). GPS plus Interferometric Synthetic Aperture Radar (InSAR) inversion of the strain field suggest that the Coyote Creek strand of the San Jacinto fault may dip northeast (Fialko, 2006). Relocated earthquakes tend to lie northeast of the mapped trace of the San Jacinto fault, and may suggest that a steep northeast dip

direction is more likely than a vertical or southwest dip. In order to distinguish between these contradictory possibilities we analyzed the spatial patterns of small earthquakes in the study area from a large dataset published by Shearer et al. (2005).

2. Methodology

2.1. Geology

Although geological maps of the Clark fault zone exist, they are incomplete, of variable scales, and document a fraction of the southeast Clark fault zone (Dibblee, 1954, 1984, 1997; Morley, 1963; Hoover, 1965; Sharp, 1967, 1972; Weismeyer, 1968; Bartholomew, 1968; Reitz, 1977; Pettinga, 1991, unpublished data; Kirby, 2005; Lutz, 2005; Steely, 2006; Dorsey, unpublished data; Janecke, unpublished data). Additional field mapping was conducted in order to produce a 1:24,000 scale structural and geological map of the southeast part of the Clark fault and to identify segments along the fault zone. The geological map is the size of ~ 2.5 USGS 7.5' quadrangle maps, and lies within the Fonts Point, Seventeen Palms, Truckhaven, Borrego Mountain, Shell Reef, and Kane Spring NW quadrangles. Three geological cross sections were produced from the compiled geological map. Stereograms of bedding orientations were made using a combination of ArcView for data selection and StereoWin to plot the data. These stereograms were used to calculate fold axes orientations and interlimb angles of the major folds and domains. Fault planes and slickenline orientations were also analyzed using stereograms.

2.2. Microseismicity

Thousands of earthquakes with magnitudes ranging between M_w 0.1 and 6.4 have been recoded in the southeast Clark fault zone. Earthquake hypocenters from the SHLK_1.0 catalog relocated by Shearer et al. (2005) occurred between 1982 and 2002. Over 6000 earthquakes with greater precision of their relative locations were extracted from this dataset. We also plotted the positions of the 1954 M_w 6.4 Arroyo Salada and 1968 M_w 6.8 Borrego Mountain earthquakes. Hypocenters in the southern California Seismic Network (SCSN) catalog with magnitudes greater than M_L 2.0 from 2005 are analyzed as well.

These data were acquired from the Shearer et al. (2005) relocation study as well as the Southern California Earthquake Center (SCEC, http://www.scec.org/). Earthquake epicenters were plotted using ArcMap software and three dimensional views of hypocenters were developed in ArcScene. Cross sections of the earthquake data were developed in Plotxsec software using the SHLK_1.01 catalog (http://www.data.scec.org/ftp/catalogs/SHLK/).

3. Results

3.1. Structural Overview of the Southeast Clark Fault Zone

As the Clark fault enters into the San Felipe-Borrego subbasin it is characterized by a southeastward broadening zone of complex deformation. The zone of deformation related to the Clark fault is defined by structures that accommodate strain associated with the Clark fault, and link or connect to the central traces of this fault. The deformation observed at the surface includes complex interactions between multiple folds and faults with highly variable orientations and kinematics. The scales of structures are highly

variable. Faults and folds may range in length from the kilometer to centimeter scale. Deformation is partitioned into domains where similar structures are concentrated in particular areas. In the southeast there is a structural boundary characterized by a zone of northeast-southwest striking sinistral-normal strike-slip faults with southeast down-dip components of slip. We refer to this as the "Pumpkin Crossing block". Strain associated with the Clark fault is also taken up by multiple folds that vary in scale throughout the entire fault zone. The deformation can be subdivided into three distinct structural segments that consist of at least 10 domains of deformation.

The Clark fault zone is ~ 1.5 km wide and has three major traces near Lute Ridge (UTM, 0574000, 3686000) in the northwest corner of the study area (Fig. 3-4, Plate 1). A central zone dominated by dextral strike-slip faults continues southeast past previous terminations of the Clark fault. The central Arroyo Salada fault traces are characterized by a 2.2 km wide zone with ~ 10 major fault traces near the Arroyo Salada pediment (UTM, 11S 0580500, 3682000). Major branch points at Lute Ridge and the Leon pediment (UTM, 11S 0578000, 3683000) link splays to the northeast and southwest. Major branches of the fault deform the sedimentary rocks by complex linkages of fault bends and stepovers. Sinistral strike-slip faults oriented northeast-southwest occur throughout most of the fault zone and approximately 15 km to the southeast of Lute Ridge a large zone of these antithetic faults cross the central zone of deformation. These faults persist for distances of 2-9 km along strike.

Evidence of contractional and extensional deformation has been documented in the southeast part of the Clark fault. Extensional north-south striking normal faults and strike-slip faults with oblique down-dip components are found throughout the field area

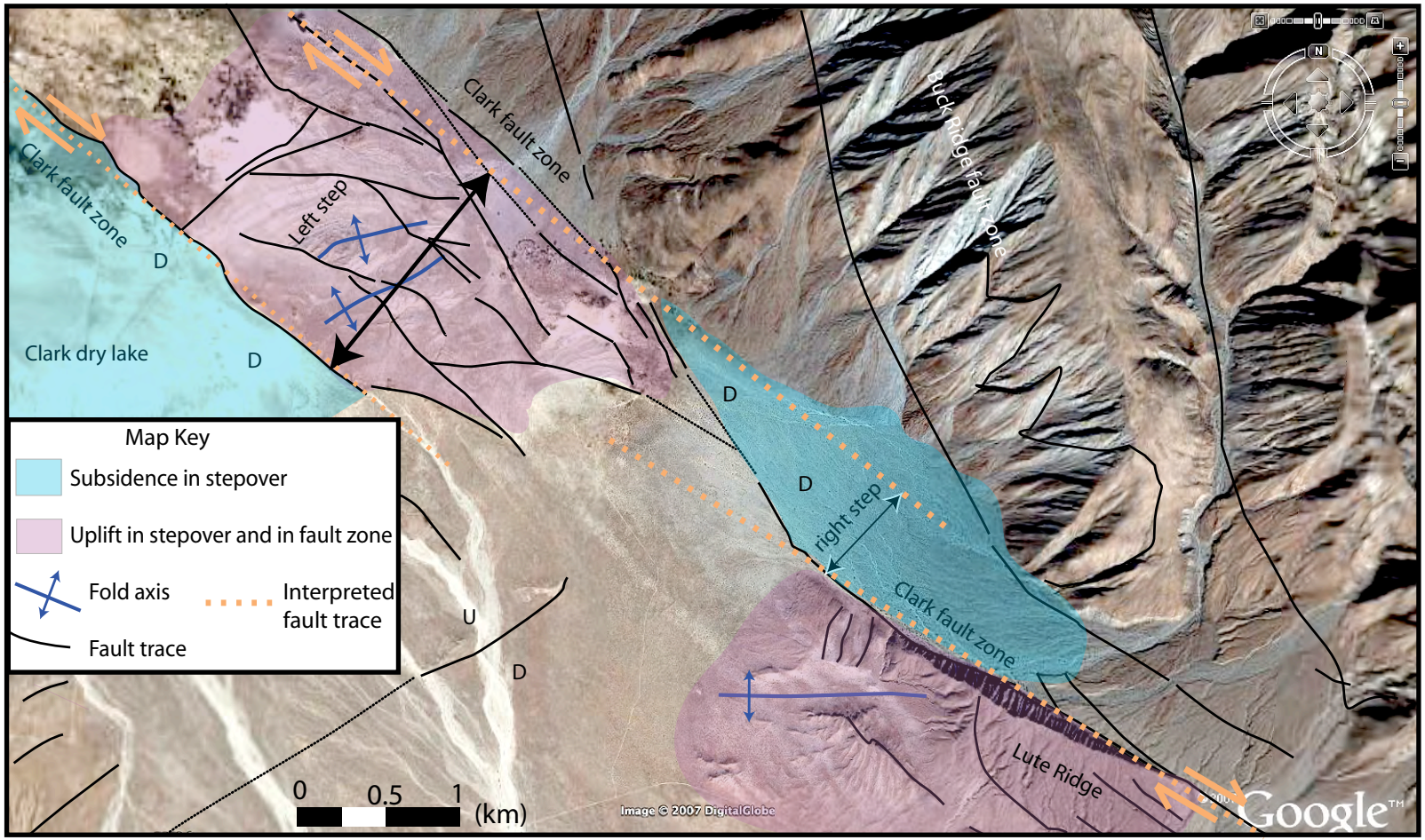

Fig. 3-4. Google Earth image and geology of the southeast part of the Santa Rosa Segment. Geological interpretation by S. Janecke. Notice the stepovers between the fault traces.

(Fig. 3-5). A concentration of normal faults is located in the northeast corner of the study area near Salton City (Plate 1). Contractional components of strain are represented by large folds northeast and southwest of the central deformation zone as well by reverse to oblique-reverse components on many east-northeast to east-southeast striking faults (Fig. 3-5). A concentration of these types of faults is located in the central part of the field are near 17 Palms (Plate 1).

With the addition of one structural segment to the southeast called the San Felipe Hills segment our structural segmentation is grossly in accordance with rupture segments postulated by Sanders (1989). Two structural boundaries partition the Clark fault into the Santa Rosa, the Arroyo Salada and the San Felipe Hills segments from northwest to southeast (Fig. 3-2). The Santa Rosa segment is identified by its relatively continuous fault traces in Clark Lake Valley and along the south-southwestern edge of the Santa Rosa Mountains (Sharp, 1967; Dorsey, 2002; Ryter, 2002; this study). Northeast of Clark Dry Lake this segment steps ~ 1.6 km left and contains 1-3 major splays within a relatively narrow deformation band ~ 2 km wide (Fig. 3-4). The main trace within this zone steps ~ 0.7 km to the right via 2 bends northwest of Lute Ridge and produces extensional strains there (Ryter, 2002; this study) (Fig. 3-4). Faulting is distributed across a 1.5 km wide zone of fault scarps for the next ~5.4 km at and southeast of Lute Ridge. Up to 9 subparallel to anastomosing fault traces offset Quaternary deposits in the fault zone (Plate 1). The southeastern boundary of the Santa Rosa segment is marked by a concentration of branch points of faults that bend away from the Clark fault towards the north and south.

Fig. 3-5.

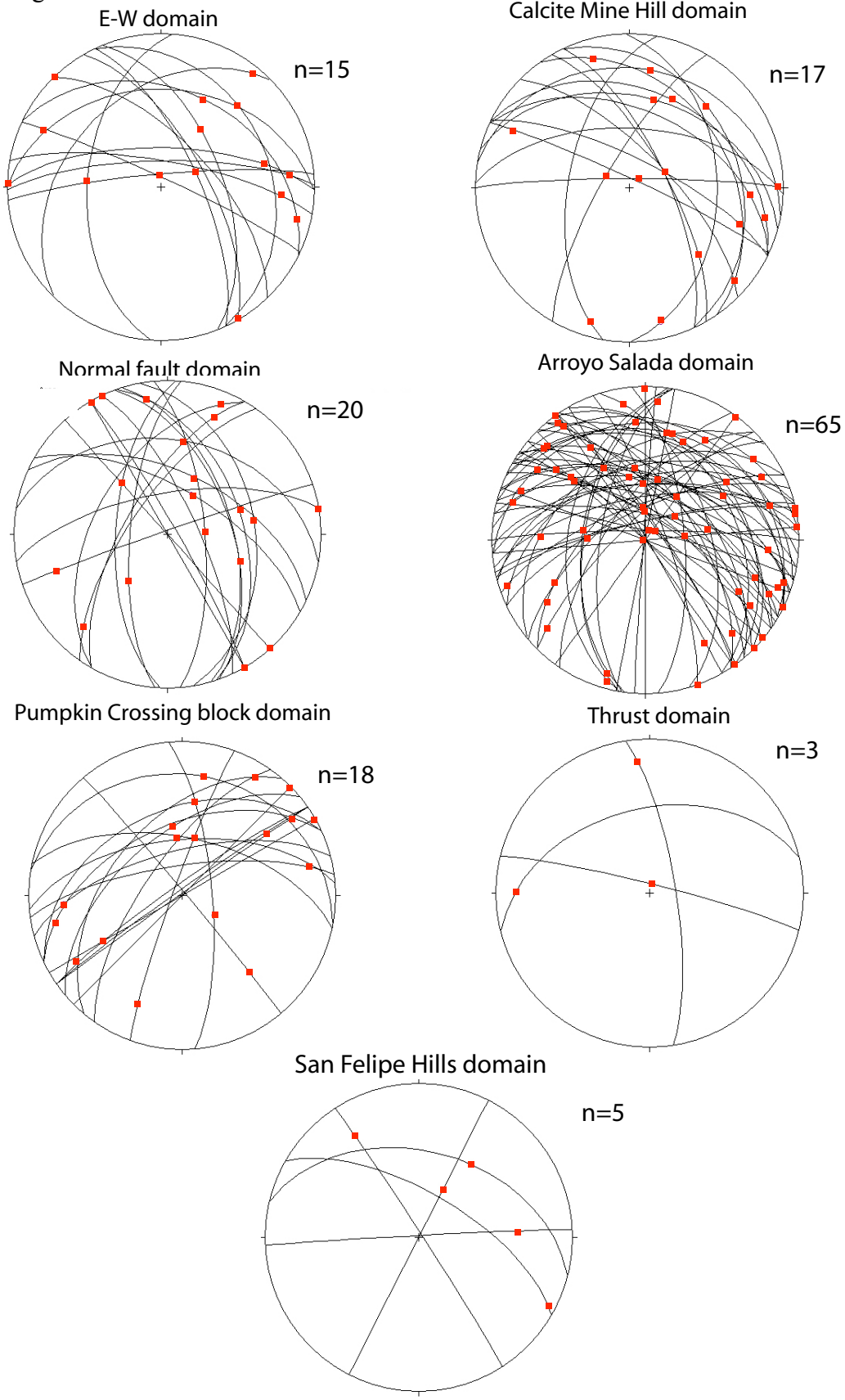
E-W domain
n=15
Calcite Mine Hill domain
n=17
Normal fault domain
n=20
Arroyo Salada domain
n=65
Pumpkin Crossing block domain
n=18
Thrust domain
n=3
San Felipe Hills domain
n=5

Fig. 3-5. Stereograms of selected fault planes with slickenlines (red boxes) within the interpreted fault domains of the Clark fault zone. Data collected by the authors. Fault domains where too few data points were collected are not included.

The Arroyo Salada segment contains a central zone of northwest-striking dextral faults as well as a broad zone with multiple off-fault structures. Large subsidiary structures associated to the Clark broaden the zone of deformation to at least ~ 18 km wide (Fig. 3-2). The Truckhaven, and San Felipe Hills faults are interpreted to be the boundaries of the Arroyo Salada segment damage zone because they are the final structures that link to and accommodate strain of the Clark fault (Fig. 3-2). Continuous faults with various faults steps and bends are characteristic of this segment. The central zone of deformation is dominated by dextral strike-slip faults along strike of those in the Santa Rosa segment. This zone has 10 major fault scarps with southwest-down sense of slip spaced ~ 100 m apart. Major folds within this segment are the northwest-trending Borrego syncline and, the east-west trending Graves Wash anticline. The southeastern boundary of this segment is the Pumpkin Crossing block in the central part of the map (Plate 1).

Deformation within the central zone of the San Felipe Hills segment is dominated by complex sets of en echelon fault zones that merge into a series of folds and faults to the southeast (e.g. Kirby et al., 2007). Sinistral strike-slip faults possibly related to the Pumpkin Crossing block that strike northeast surround the central San Felipe Hills fault zone. The San Felipe Hill segment is present in much of the San Felipe Hills and is the southeastern most segment of the Clark fault. The boundary to the southeast is the ~ 5 km wide Extra fault zone (Kirby, 2005; Janecke, unpublished mapping) (Fig. 3-2).

3.2. Subsidiary Structures

Structures that account for major parts of the separation or shortening within the Arroyo Salada and San Felipe Hills segments are identified on plates 1, and 2, and

described below as well as in table 3-1. Although a few of these structures have been previously documented (Dibblee, 1954; Hoover, 1965; Sharp, 1967, 1972, 1975; Weismeyer, 1968; Bartholomew, 1968; Reitz, 1977; Wells, 1987; Kirby, 2005; Lutz, 2005; Steely, 2006), additional data collected in this study has characterized the following structures in greater detail.

There are nine large faults and five major folds that accommodate a major part of the strain associated to the Clark fault. In general there is interference between the subsidiary structures within the southeast part of the Clark fault zone. Interference is also developed among minor structures in the fold and fault domains of the Clark fault zone (Fig. 3-6, 3-7). Due to these complex relationships, very few cross-cutting relationships provide meaningful insight towards a sequence of events within the whole fault zone.

3.2.1. Faults

The central Clark fault zone is dominated by a 1.5 km wide band of subparallel to anastomozing dextral reverse faults that strike between 115° - 140° (Fig. 3-7). This band of faults continues ~9-10 km to the southeast of county road S22. These faults displace Pleistocene to Holocene (?) deposits of the Arroyo Salada pediment producing 1-3 m high fault scarps that are dominated by southwest-down components (Plate 2). The faults continue to the northwest and southeast of the scarps in the bedrock along bedding planes and are difficult to find in the field unless exposure is excellent. Ramp-flat geometries cross bedding planes are well exposed along these faults near the southern end of Coachwhip Canyon (Fig. 3-8). The faults at the surface dip moderately to steeply towards the southwest (Plate 1). Slickenlines are subhorizontal and show a major strike-

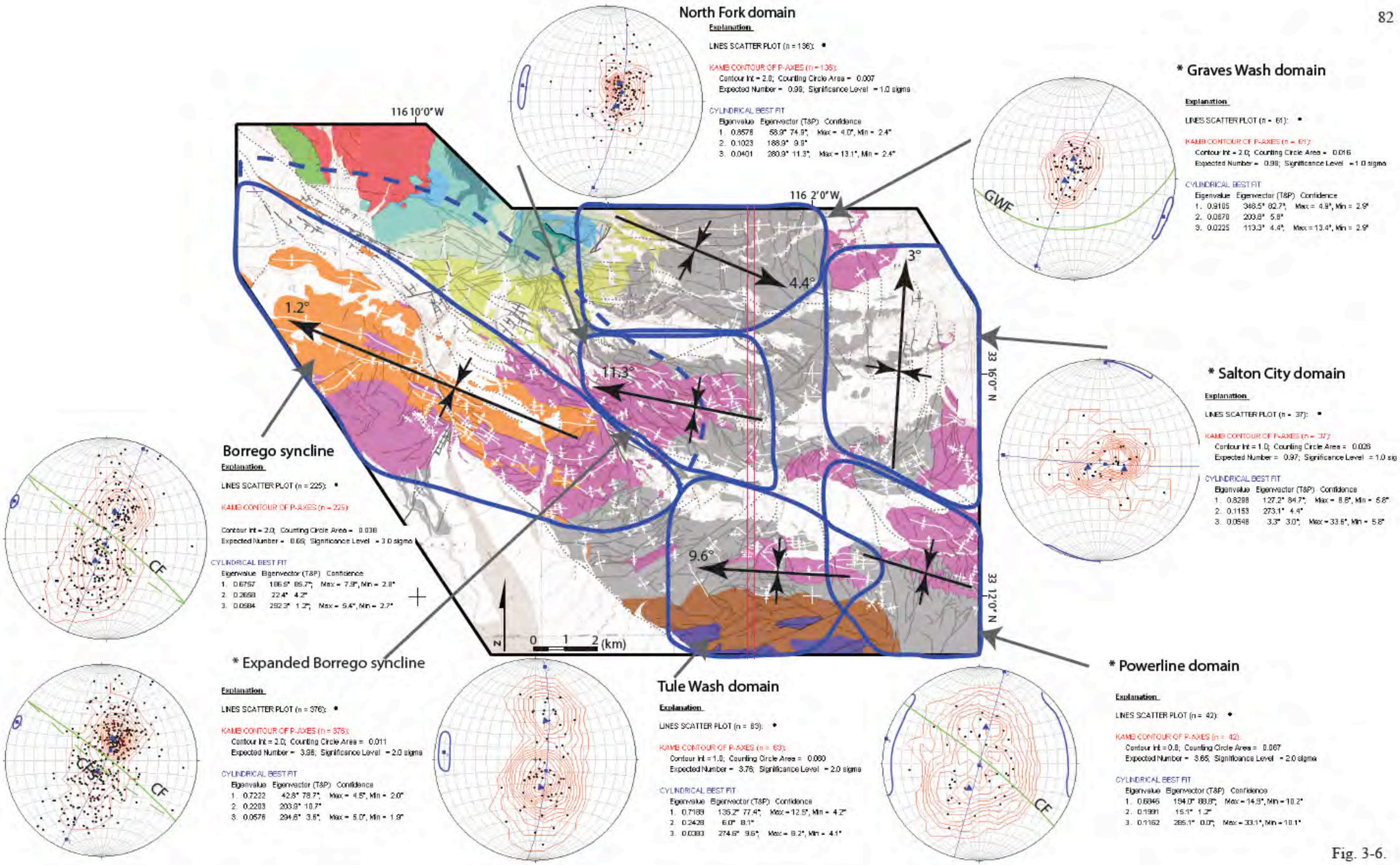
North Fork domain
Explanation
LINES SCATTER PLOT (n = 136):
KAMB CONTOUR OF P-AXES (n = 136):
Contour Int = 2.0; Counting Circle Area = 0.007
Expected Number = 0.98; Significance Level = 1.0 sigma
CYLINDRICAL BEST FIT
Eigenvalue Eigenvector (T&P) Confidence
1. 0.8578 58.9° 74.9°; Max = 4.0°, Min = 2.4°
2. 0.1023 188.9° 9.8°
3. 0.0401 280.9° 11.3°; Max = 13.1°, Min = 2.4°
* Graves Wash domain
Explanation
LINES SCATTER PLOT (n = 61):
KAMB CONTOUR OF P-AXES (n = 61):
Contour Int = 2.0; Counting Circle Area = 0.016
Expected Number = 0.98; Significance Level = 1.0 sigma
CYLINDRICAL BEST FIT
Eigenvalue Eigenvector (T&P) Confidence
1. 0.9105 346.5° 82.7°; Max = 4.9°, Min = 2.9°
2. 0.0870 209.8° 5.8°
3. 0.0225 119.3° 4.4°; Max = 13.4°, Min = 2.9°
GWF
116 10'0" W
116 2'0" W
33 16'0" N
33 12'0" N
1.2°
4.4°
11.3°
3°
9.6°
N
0 1 2 (km)
Borrego syncline
Explanation
LINES SCATTER PLOT (n = 225):
KAMB CONTOUR OF P-AXES (n = 225):
Contour Int = 2.0; Counting Circle Area = 0.036
Expected Number = 8.65; Significance Level = 3.0 sigma
CYLINDRICAL BEST FIT
Eigenvalue Eigenvector (T&P) Confidence
1. 0.6757 186.5° 85.7°; Max = 7.9°, Min = 2.8°
2. 0.2658 22.4° 4.2°
3. 0.0584 292.3° 1.2°; Max = 5.4°, Min = 2.7°
CF
* Salton City domain
Explanation
LINES SCATTER PLOT (n = 37):
KAMB CONTOUR OF P-AXES (n = 37):
Contour Int = 1.0; Counting Circle Area = 0.026
Expected Number = 0.97; Significance Level = 1.0 sig
CYLINDRICAL BEST FIT
Eigenvalue Eigenvector (T&P) Confidence
1. 0.8288 127.2° 84.7°; Max = 8.8°, Min = 5.8°
2. 0.1153 273.1° 4.4°
3. 0.0548 3.3° 3.0°; Max = 33.6°, Min = 5.8°
* Expanded Borrego syncline
Explanation
LINES SCATTER PLOT (n = 376):
KAMB CONTOUR OF P-AXES (n = 376):
Contour Int = 2.0; Counting Circle Area = 0.011
Expected Number = 3.98; Significance Level = 2.0 sigma
CYLINDRICAL BEST FIT
Eigenvalue Eigenvector (T&P) Confidence
1. 0.7222 42.8° 78.7°; Max = 4.5°, Min = 2.0°
2. 0.2203 203.9° 10.7°
3. 0.0576 294.6° 3.6°; Max = 5.0°, Min = 1.9°
CF
Tule Wash domain
Explanation
LINES SCATTER PLOT (n = 83):
KAMB CONTOUR OF P-AXES (n = 83):
Contour Int = 1.0; Counting Circle Area = 0.060
Expected Number = 3.76; Significance Level = 2.0 sigma
CYLINDRICAL BEST FIT
Eigenvalue Eigenvector (T&P) Confidence
1. 0.7189 135.2° 77.4°; Max = 12.5°, Min = 4.2°
2. 0.2428 6.0° 8.1°
3. 0.0383 274.6° 9.6°; Max = 8.2°, Min = 4.1°
* Powerline domain
Explanation
LINES SCATTER PLOT (n = 42):
KAMB CONTOUR OF P-AXES (n = 42):
Contour Int = 0.8; Counting Circle Area = 0.067
Expected Number = 3.65; Significance Level = 2.0 sigma
CYLINDRICAL BEST FIT
Eigenvalue Eigenvector (T&P) Confidence
1. 0.6845 154.0° 88.8°; Max = 14.5°, Min = 10.2°
2. 0.1991 15.1° 1.2°
3. 0.1162 285.1° 0.0°; Max = 33.1°, Min = 10.1°
CF

Fig. 3-6.

Fig. 3-6. Fold domains of the Clark fault zone. Refer to plate 1 for the key to the geological map in the background. Formations younger than the Ocotillo Formation are white on the map. Black arrows show the dominant trend and plunge of folds in each domain. Blue lines are the domain boundaries. Red lines are the north-south transect. Blue dashed line is northern boundary of the Expanded Borrego syncline domain. Note that the Kamb contour intervals vary amount the stereograms. Average fold limbs depicted where blue triangles intersect the cylindrical best fit lines. Blue square is average trend and plunge in each fold domain with error ovals, Green lines show major fault planes, CF: Clark fault, CFS: Clark fault trace in the subsurface, GWF: Graves Wash fault. The asterisks (*) indicate folds discussed in section *3.2.2.*

Fig. 3-7.

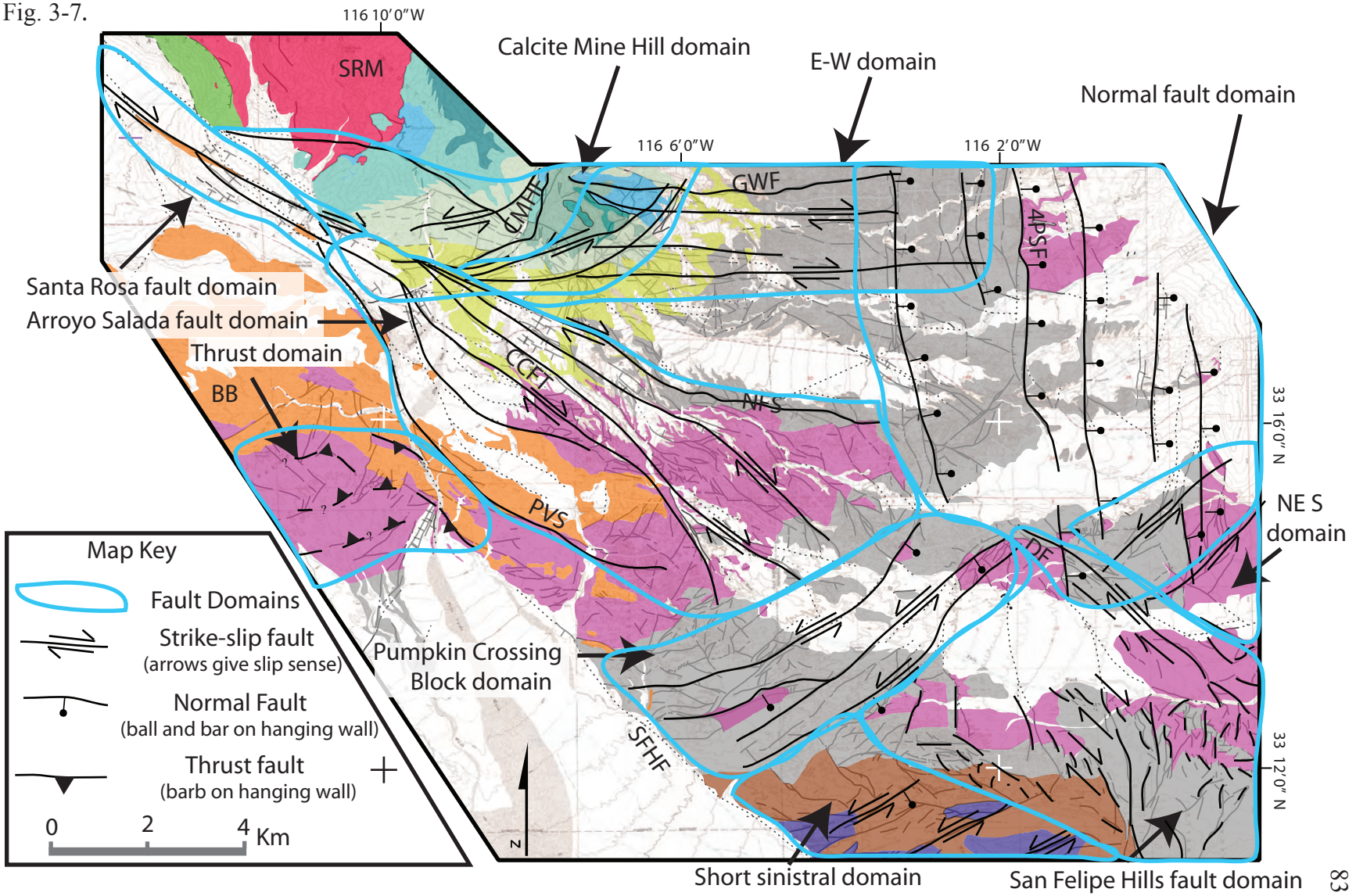
116 10′ 0″W
116 6′ 0″W
116 2′ 0″W
33 16′ 0″ N
33 12′ 0″ N
SRM
Calcite Mine Hill domain
E-W domain
Normal fault domain
GWF
CMHF
4PSF
Santa Rosa fault domain
Arroyo Salada fault domain
Thrust domain
BB
CCFT
NFS
PVS
DF
NE S
domain
Pumpkin Crossing
Block domain
SFHF
Short sinistral domain
San Felipe Hills fault domain
Map Key
Fault Domains
Strike-slip fault
(arrows give slip sense)
Normal Fault
(ball and bar on hanging wall)
Thrust fault
(barb on hanging wall)
0
2
4 Km
N

Fig. 3-7. Fault domains of the Clark fault zone. Refer to plate 1 for the key to the geological map in the background. ions younger than the Ocotillo Formation are white. Major structures that characterize each domain are indicated I black. Note that most fault domains overlap. SFHF- San Felipe Hills fault; NE S- NE sinistral domain; PVS- Palo Verde Splay; NFS- North Fork Splay; CCFT- Central Clark fault trace, BB- Borrego Badlands; SRM- Santa Rosa Mountains; GWF- Graves Wash fault; 4PSF- Four Palms Spring fault; DF- Dump fault; CMHF- Calcite Mine Hill fault.

Fig. 3-8.

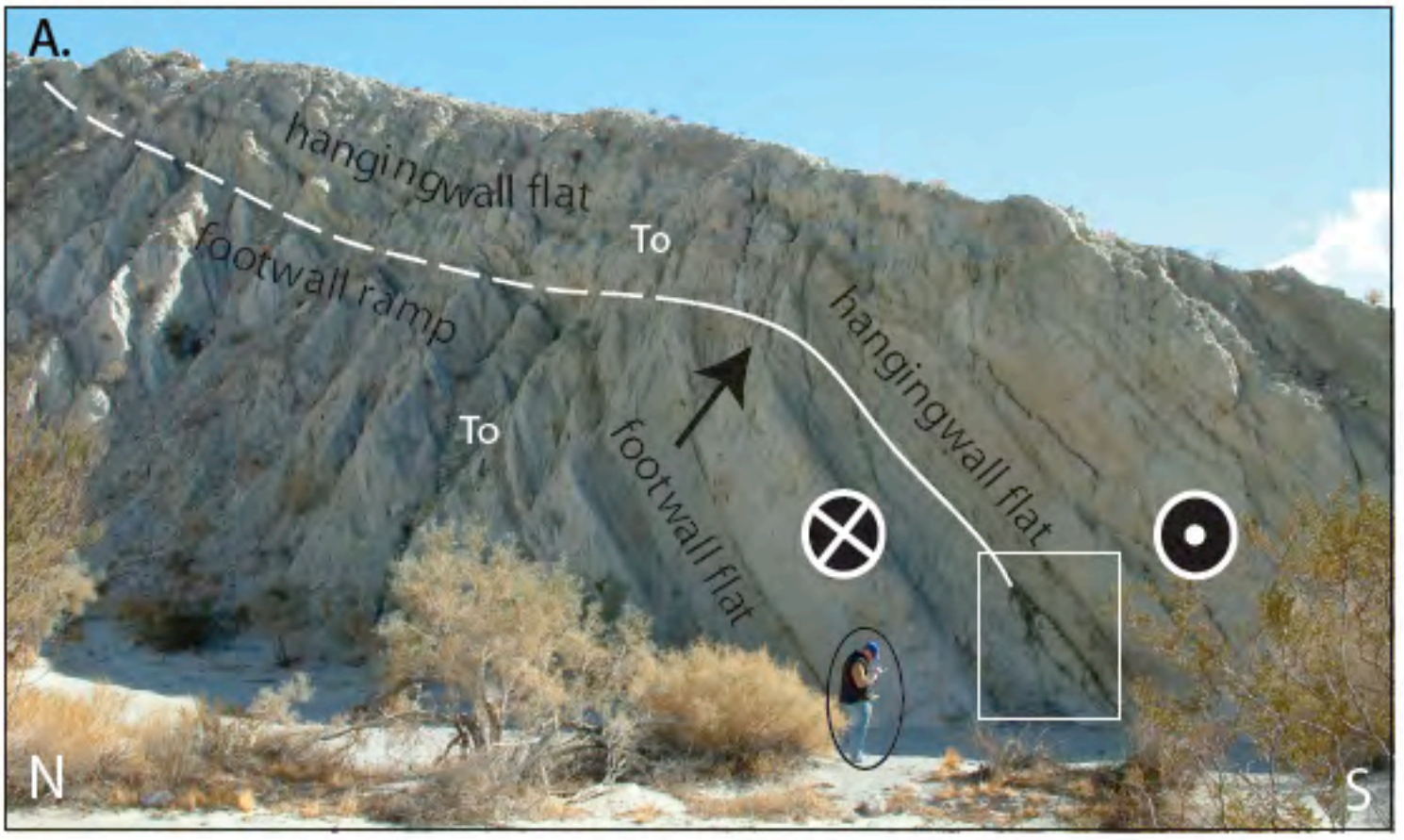
A.
hangingwall flat
To
footwall ramp
To
footwall flat
hangingwall flat
N
S


B.


C.

Fig. 3-8. Photographs of bedding parallel faults on the east side of Coachwhip Canyon (UTM 11S, 579321, 3683572). This fault is a major strand in the central Clark fault zone and has a scarp ~ 1.2 km to the southeast on the Arroyo Salada pediment. The fault plane is 124°, 63° SW and the slickenlines trend 289 °. Bedding of the Olla Formation (To) strikes and dips 124°, 48° SW. (A) Photograph looking east-southeast at a bedding parallel strike-slip fault with a ramp flat geometry. White line: Main fault trace, Red line: Fault damage zone, White box: outline of B and C, 6' person for scale. Black arrow indicates the transition between footwall ramp and the footwall flat. (B) Close-up photograph of fault zone 40 cm hammer for scale. (C) Blue lines: bedding parallel faults, Red lines: fault ramps across bedding, Blue pattern: gouge area of intense deformation.

Geological Structures of the San Felipe Hills, Borrego Badlands, and Santa Rosa Mountains

Folds	Orientation	trend	plunge	%N-S Shortening	1/2 Wavelength (km)	Interlimb angle	Age of activity*	Source
Fold Domains								
*Graves Wash	E-W	113 ± 13°	4± 3°	2.30%	4.3	162°	Borrego Fm	
*Expanded Borrego syncline	NW-SE	294 ± 5°	4 ± 2°	4.10%	7.7	149.5°	Quaternary alluvium	
*Salton City	N-S	3 ± 33°	3 ± 5°	2.20%	4.4	151.4°	Ocotillo/Brawley Fm	
Borrego syncline	NW-SE	292 ± 5°	1 ± 3°	12.50%	5.4	122.5°	Quaternary alluvium	
North Fork	E-W	281 ± 13°	11 ± 2°	4.90%	3.9	146.4°	Borrego Fm	
Tule Wash	E-W	274 ± 8°	10 ± 4°	15.80%	4.8	116.4°	Borrego Fm	
*Powerline	NW-SE	285 ± 33°	0 ± 10°	11.20%	4.6	127.3°	Ocotillo/Brawley Fm Quaternary?	
Adjacent folds								
San Felipe Hills anticline	E-W	87± 4°	0± 5 °		10		~1.1 to ~0.5 Ma (1)	Kirby et al., 2007

Faults	Orientation	strike	dip	Separation	Length	Throw, Type	Age of activity*	Source
Larger faults within the								
Clark fault zone								
Complex en echelon fault zone	NW-SE	126°	Steep E	U RS		NE side down,S-S Oblique		
Four Palm Spring fault	N-S	000°	67° E	~0.3 km V	10-12 km	E side down, Normal	Borrego Fm	L = Weismeyer 1968
Western Calcite Mine Hill fault	NNE-SW	019°	Steep E	> 0.2 km V		E side up, Reverse	Pleistocene-Holocene alluvium	
Central Clark fault zone	NW-SE	309°	83° NE	5.62 - 18 km	8 km	NE side up, S-S Oblique	Pleistocene-Holocene alluvium	L=Avg. along strike first NW
Graves Wash fault	E-W	075°	49° S	> 0.2 km V	9-U km	S side up, Reverse	Borrego or ?Brawley? Fm	L= Used Weismeyer 1968
San Felipe Hills fault	NW-SE	316°	~90°	2.5 km RS (This Study)	15-16 km	S side down, S-S	Ocotillo Fm	L=Dibblee 1954
Powerline fault	NW-SE	140°	~90°		8-12 km	S-S	Ocotillo/Brawley Fm	Kirby 2005
Pumpkin Crossing Block	NE-SW	51°	72° SE	1 km V U LS	7.3 km	SE down, S-S Normal	Pleistocene-Holocene alluvium	
North Fork splay	E-W				10.4 km	S-S, N side up reverse	Pleistocene-Holocene alluvium	
Palo Verde splay	NW-SE	161°	61-90° SE		10.6 km	S-S	Pleistocene-Holocene alluvium	
Adjacent Faults								
Santa Rosa fault	NW-SE	150°	~75° SW	6 km RS (Sharp 1967)	27 km	S-S		Sharp 1967, Sanders 1989
Anza Segment, Clark fault	NW-SE	124°	Steep	24 km RS (Sharp 1967)	25-30 km	S-S		L=Sanders 1989
Santa Rosa Segment, Clark fault	NW-SE	300°	83° NE	18 km RS (Sharp 1967)	12 km	S-S		L=Sanders 1989
Coyote Creek fault	NW-SE	313°	~90°-NE	1-4.8 km RS (Sharp, 1967)	80-90 Km	S-S		L=Sharp 1967
Extra fault zone	ENE-WSW	47°	60-90° NW	U LS	40-50 Km	S-S		Hudnut et al., 1989; Kirby, 2005

***Major Folds highlighted in section 3.2.2.**

U = undetermined
RS = right separation
V = vertical

S-S = strike slip (1) lessor growth since then
Age of activity* = Youngest feature defromed by this structure

Table 3-1. Table of major structures in the region and structural domains of the southeast Clark fault zone.

slip component with minor oblique components (Plate 1). Total right-separation along these bedding-strike-parallel faults was indeterminable.

Major splays branch off the central faults of the Clark fault southeast of Lute Ridge. The Palo Verde splay branches southward where the central trace of the Clark fault intersects Palo Verde Wash. This splay strikes ~ 161° and dips southwest between 61° to 90° (Plate 1). Evidence of this fault is found along the west side of Palo Verde Wash where it juxtaposes Borrego type mudstones to the east against Ocotillo Formation to the west. The northern part of the fault is primarily strike-slip with slickenlines of nearly 90° rakes (Plate 1). This fault takes a concave-northeast bend near the confluence of Ella and Palo Verde Washes, and follows the Ocotillo Borrego contact east for ~ 6 km. The eastern end of this splay is truncated by northeast-striking sinistral-oblique faults near Basin Wash (Plate 1).

Another major splay, the North Fork splay, branches eastward from the Arroyo Salada central fault traces near the intersection of the Arroyo Salada Wash and the central Clark fault (Plate 1). The North Fork splay strikes ~ 95° along the southern edge of the Tower pediment (Plate 1). This fault is characterized by a series of fault planes with similar strikes but variable dips and dip directions of 64° - 80° S, 55° - 70° N. Slickenlines are highly variable ranging from vertical to nearly horizontal along these fault strands indicating variable kinematics (Plate 1). The westernmost part of this fault branches off the central Clark fault zone as a nearly vertical dextral strike-slip fault (Plate 3, A-A'). As the fault bends towards the east near the Tower pediment the fault is moderately dipping towards the north with reverse components of slip(Plate 3, B-B'). Along this part of the fault overturned folds parallel the fault in its footwall. Smaller fault

planes near this splay have strike-parallel slickenlines that suggest a strike-slip component.

The Western Calcite Mine Hill fault is a sinistral-reverse fault just west of Calcite Mine Hill (Dibblee, 1954, 1984; Hoover, 1965; Weismeyer, 1968; Bartholomew, 1968; this study). The fault strikes ~ 20° and dips steeply towards the east (Plate 1). Several east-west striking dextral faults cut across and segment the southwest end of the Western Calcite Mine Hill fault. The southwest end may splay from the Arroyo Salada central fault traces at the same branch point as the North Fork splay. The northern part of this fault bends to an east-northeast strike and may link to the Truckhaven fault farther to the north near Travertine Ridge (Janecke, unpublished mapping) (Fig. 3-2). The Western Calcite Mine Hill fault vertically offsets various units of the Canebrake Conglomerate and the Calcite Mine megabreccia > 0.2 km near Calcite Mine Hill. The Graves Wash fault branches east from the Western Calcite Mine Hill fault near its midpoint (Plate 1).

The Dump fault previously document by Kirby (2005) is a dextral strike-slip fault in the northwest part of the San Felipe Hills segment. This fault is a nearly vertical fault that strikes ~118°. This fault is the northern contact of a down-dropped block of Borrego Formation and the south edge of the transitional unit. Components of oblique southeast-side-down slip on the Pumpkin Crossing block also faulted this Borrego block into place. The Dump fault may be linked to the southeast end of the North Fork splay by an extensional stepover, or it may be a southeast continuation of the central Arroyo Salada fault traces displaced left laterally by the Pumpkin Crossing block. The Dump fault dies out to the southeast into a complex zone of faults and folds in the southeasternmost part of the study area (Plate 1).

The Four Palms Spring fault located in the east-northeast part of the study area is an east-dipping normal fault that down-drops the Borrego Formation on the east (Plate 1). This fault has poor surface exposures in Palm Wash but similarly oriented faults in this area dip moderately east ~ 67°. This fault continues for at least 10 km to the north. To the south this fault bends eastward and is covered by young alluvium near Tectonic Gorge. There is ~ 0.3 km of vertical offset along this fault (Weismeyer, 1968; this study).

To the north of the study area the Four Palms Spring fault truncates the east-west striking Graves Wash fault (Eckis, 1930; Dibblee, 1954; Weismeyer, 1968; this study). The Graves Wash fault is a steeply to moderately south-dipping fault with a reverse component inferred from the juxtaposition of Canebrake Conglomerate (Tc3) and Split Mountain megabreccia north of Calcite Mine Hill (Plate 1). The Graves Wash fault located in the northern part of the study area has ~ 0.5 km of vertical offset (Plate 3, B-B'). Minor amounts of normal slip are inferred in the east because normal drag folding is consistently preserved in the hanging wall in several excellent exposures of the fault (Fig. 3-9).

The San Felipe Hills fault strikes ~ 142 ° along the northeastern edge of the Quaternary alluvium in the southwestern part of the study area. The poorly exposed San Felipe Hills fault dips 44- 74 ° to the northeast near Palo Verde Wash where it bends west into the Borrego Badlands (Plate 3, A-A'). The transitional unit is displaced ~ 2.5 km right laterally in the southwest part of the study area across the San Felipe Hills fault (Plate 1). A southwest-side down component of slip across this fault diverts Quaternary streams to the southwest side of this fault. The San Felipe Hills fault is described below as a dextral strike-slip fault that is a subsidiary fault within the Clark fault zone but the

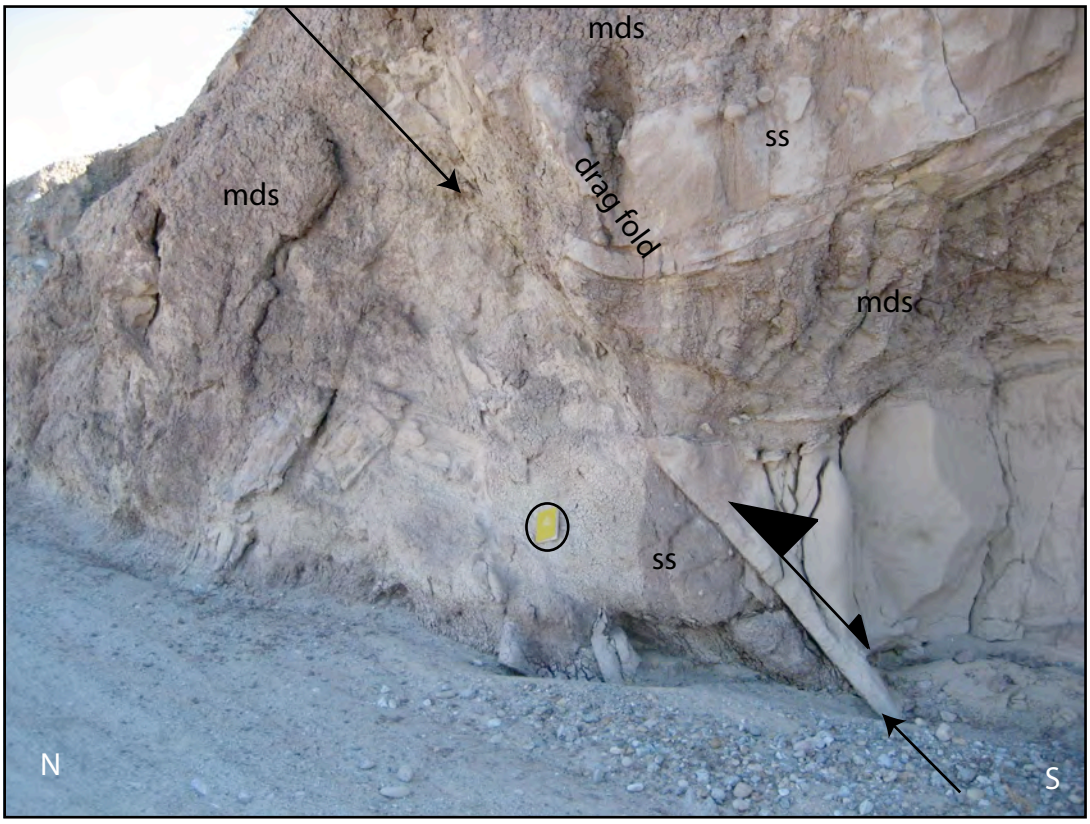

Fig. 3-9. Photograph looking west at the Graves Wash fault in Graves Wash indicate by the black arrows (UTM 11S, 0590159, 3686042). The strike and dips of the fault is 089°, 46° S. Slickenlines trend ~190°. The rocks are altered mudstones (mds) and sandstones (ss) of the Transitional Formation. The Graves Wash fault has a major reverse component because it places older rocks on younger rocks at Calcite Mine Hill. The minor drag fold caused by a secondary normal component slip. A 20 cm long yellow book for scale.

linkage of strain between the Clark fault zone and the Coyote Creek fault zone to the south is unclear.

The Truckhaven fault is a northeast-southwest striking normal fault at the southeast side of Travertine Ridge (Eckis, 1930; Dibblee, 1954; Weismeyer, 1968) (Fig. 3-2). The basement rocks of Travertine Ridge exposed in the footwall of this fault are juxtaposed against upper Canebrake Conglomerate to the southeast. This fault may have a reverse and or strike-slip component as well (Janecke, unpublished). We suggest that the Truckhaven fault is the northern boundary of the Clark fault zone but future work needs to be done in order to better constrain this.

There are a series of crossing faults in the Pumpkin Crossing block that form a structural boundary between the Arroyo Salada and San Felipe Hills segments. These faults are northeast-southwest trending sinistral strike-slip faults with an oblique-normal component (Plate 1). Five major faults within the crossing block series repeat sections of the Borrego Formation and reflect some southeast-side-down displacement (Plate 3, B-B'). The southwest ends of these faults bend westward and end at or are truncated by the San Felipe Hills fault. We speculate that these faults connect with the north-south striking normal faults in the northeast but there is little to no exposure of these critical relationships.

3.2.2. Folds

The Borrego syncline is a major map-scale syncline in the western part of the study area (Dibblee, 1954; Bartholomew, 1968; Lutz, 2005; Kirby, 2005; this study) (Plate 1, Plate 3, A-A'). The Borrego syncline is a gentle fold that is cored by the Ocotillo Formation and Quaternary alluvium. The fold axis plunges 4 ± 2° toward 294 ±

5°. The trend of the Borrego syncline is subparallel to the Clark fault and trends 15° counterclockwise off the Arroyo Salada central fault traces. Below we describe evidence that shows that the Borrego syncline is currently an active fold. The northern limb of the Borrego syncline was cut off by the central Clark fault but southwest dipping beds persists northeast of the Clark fault in the Santa Rosa Mountains (Plate 3, A-A'). We include these rocks of the Olla and Canebrake formations northeast of the Clark fault in the analysis of the Borrego syncline. These data show that beds in the Arroyo Salada segment and the Santa Rosa segment generally strike parallel to the central faults of the Clark fault zone.

The east end of the single axial trace of the Borrego syncline ends or is truncated by strands of the Clark fault near 17 Palms. The axial trace splits into multiple smaller folds towards the west in the northeast Borrego Badlands west of the Palo Verde splay (Dibblee, 1954; Bartholomew, 1968; Lutz, 2005; this study). The southeast part of the fold, east of the Palo Verde splay has one central axis whereas west of this fault there are 5 subparallel anticlines and synclines. About 0.6 km of shortening is measured perpendicular to the major axial trace from the northernmost part of Arroyo Salada Wash to the southwest edge of the study area near Fault Wash.

The large east-west trending anticline north of Graves Wash and the north-northwest trending fold near the east edge of the study area was named the Santa Rosa anticline by Dibblee (1954). This anticline correlates to a basement high interpreted from similarly oriented isostatic gravity high (Kirby, 2005; Kirby et al., 2007). We redefine the Santa Rosa anticline as four separate folds, the Santa Rosa, Graves Wash, Salton City and Powerline anticlines because one continuous fold is not observed at the surface. The

Santa Rosa anticline is the northwesternmost part of Dibblee's (1954) fold and its existence was not verified.

We use the nomenclature of Weismeyer (1968) and refer to the east-west trending fold that follows Graves Wash as the Graves Wash anticline and exposes the transitional unit in its core. This a gentle fold with north and south limbs dipping ~15° and ~7° respectively (Plate 3, B-B') with a simple horizontal axis that trends ~87° (Plate 1). The Graves Wash fold domain suggests an axial trend oriented farther south at ~ 113° (Fig. 3-6), but because this domain has limited data on the north limb we suggest that the map trace is a better representation of the fold axis.

The Salton City anticline is the gentle north-northwest trending anticline that exposes the transitional unit in its core (Fig. 3-6). The east and west limbs of this fold dip ~9°, and ~20°, respectively. The northern part of this fold bends towards the west and ends or is truncated by the Four Palms Spring fault. The southern part of this fold is a dome produced by interfering northeast and northwest trending anticlines northeast of the Imperial county dump. The Salton City section of the anticline is incompletely mapped and has Quaternary cover obscuring much of its trace.

The Powerline anticline is a faulted fold that trends northwest-southeast in the southeast part of the field area near Tule Wash. This fold is highly deformed by the San Felipe Hills fault domain but is clearly a very broad northwest plunging anticline parallel to and northeast of the Powerline fault (Fig. 3-6). The northern end of the anticline ends at the Dump fault.

3.3. Structural Domains

Within the southeast portion of the Clark fault we have documented a large amount of dextral strike-slip, sinistrial strike-slip, reverse, normal and oblique faults as well as anticline and syncline folds oriented in multiple different directions. Many of these structures are concentrated in areas so subdivisions have been made where structures of particular orientations and kinematics can be picked. The interactions, interferences, spatial distributions, and relationships between these structural domains have provided useful insights towards the structural characteristics of this fault zone.

3.3.1. Fold domains

Although each of the 6 fold domains contain map-scale folds with complex geometries, dominant styles and orientations are used to characterize these domains (Fig. 3-6). All orientation data within the boundaries in fig. 3-6 are included in the stereograms. The interlimb angle, trend and plunge, half wavelength and percent shortening of each domain are summarized in (Table 3-1). The Graves Wash, Expanded Borrego syncline, Salton City, and Powerline domains help characterize our interpretations of the major folds in the Clark fault zone. Individual folds within the domains vary in sizes from meter- to kilometer-long half wavelengths and vary in style from kink to cylindrical folds. There is an estimated 1.14 km of pure north-south shortening across the three central domains (Fig. 3-6, red line). The Borrego syncline accounts for ~ 0.33 km of shortening perpendicular to the Clark fault and the Salton City domain accounts for ~ 0.1 km of east-west shortening.

The Borrego syncline was analyzed in the Borrego syncline and Expanded Borrego syncline fold domains (Fig. 3-6). These fold domains are areas where the

Borrego syncline or similarly oriented folds dominate. The Borrego syncline fold domain includes the area to the southwest of the central Clark fault zone, and the Expanded Borrego syncline fold domain includes the beds to the northeast in the Santa Rosa Mountains. These data show fold axes with trends of 294 ± 5° and 292 ± 5° which are identical within error, but the north-northeast shortening analysis varies from 12.5% to 4.1% due to their lateral extents (Table 3-1).

The Tule Wash domain is dominated by east-west-trending folds but also contains gently northwest-plunging folds (Fig. 3-6). Many small kink folds with half wavelengths < 100 m characterize this domain. There is a large west-plunging box syncline and a gentle to open syncline cored by the Borrego Formation in this domain. On average folds are open and have interlimb angles of 116°. There is approximately 0.9 km or 15.8 % of north-south shortening across this domain. This is the greatest shortening percentage in the study area (Table 3-1).

The Powerline fold domain is dominated by northwest-southeast trending folds and contains the Powerline anticline, which is the southeast end of Dibblee's (1954) Santa Rosa anticline. Many smaller kink folds with half wavelengths of < 100 m are also incorporated into this domain. This northwest-plunging anticline is faulted but still well expressed in the dipping beds. The domain is defined by a gently northwest- trending fold axis ~ 25 ° counterclockwise of the central traces of the Clark fault zone and has 11.2% northeast-southwest shortening.

The Salton City fold domain along the east side of the study area is dominated by the Salton City anticline. Most of the area is obscured by little deformed alluvial sediments. The wide scatter of poles to planes is caused by the highly variable trend of

folds near the southern boundary of this domain. This domain contains some north-south-trending folds that are drag folds above east-dipping normal faults. The average trend and plunge of folds in this domain is 3 ± 33°, 3 ± 5° and there is 2.2 % east-west shortening.

The North Fork fold domain is located south of the Tower pediment in the central part of the study area. This domain contains a gently west-southwest-plunging syncline with Borrego Formation exposed in its core. There are also several west-northwest trending folds axis that parallel strands of the Clark fault. This fold domain is similar to the eastern end of the Borrego syncline but it lies northeast of the main strands of the Clark fault zone and trends obliquely to the Borrego syncline. This domain accounts for ~ 0.2 km or 4.9 % of north-south shortening.

The Graves Wash fold domain is the area in the hanging wall of the south-dipping reverse Graves Wash fault. The main fold is a gently folded anticline plunging towards the southeast with 2.3 % north-northeast shortening. The average fold trend in this fold domain differs from that of the mapped Graves Wash anticline because a large amount of data on the northern limb is not included in our analyses.

3.3.2. Fault domains

Faults with similar geometries and kinematics are concentrated in different parts of the Clark fault zone and ar separated into 10 fault domains (Fig. 3-5, 3-7, 3-10). Most domains have one dominant type of fault, but there is much complexity and most domains contain several kinds and orientations of faults (Fig. 3-10). A few domains contain older faults cut by younger faults but most of the fault zone has mutual interactions between dextral, sinistral, oblique, and normal faults.

Fig. 3-10.

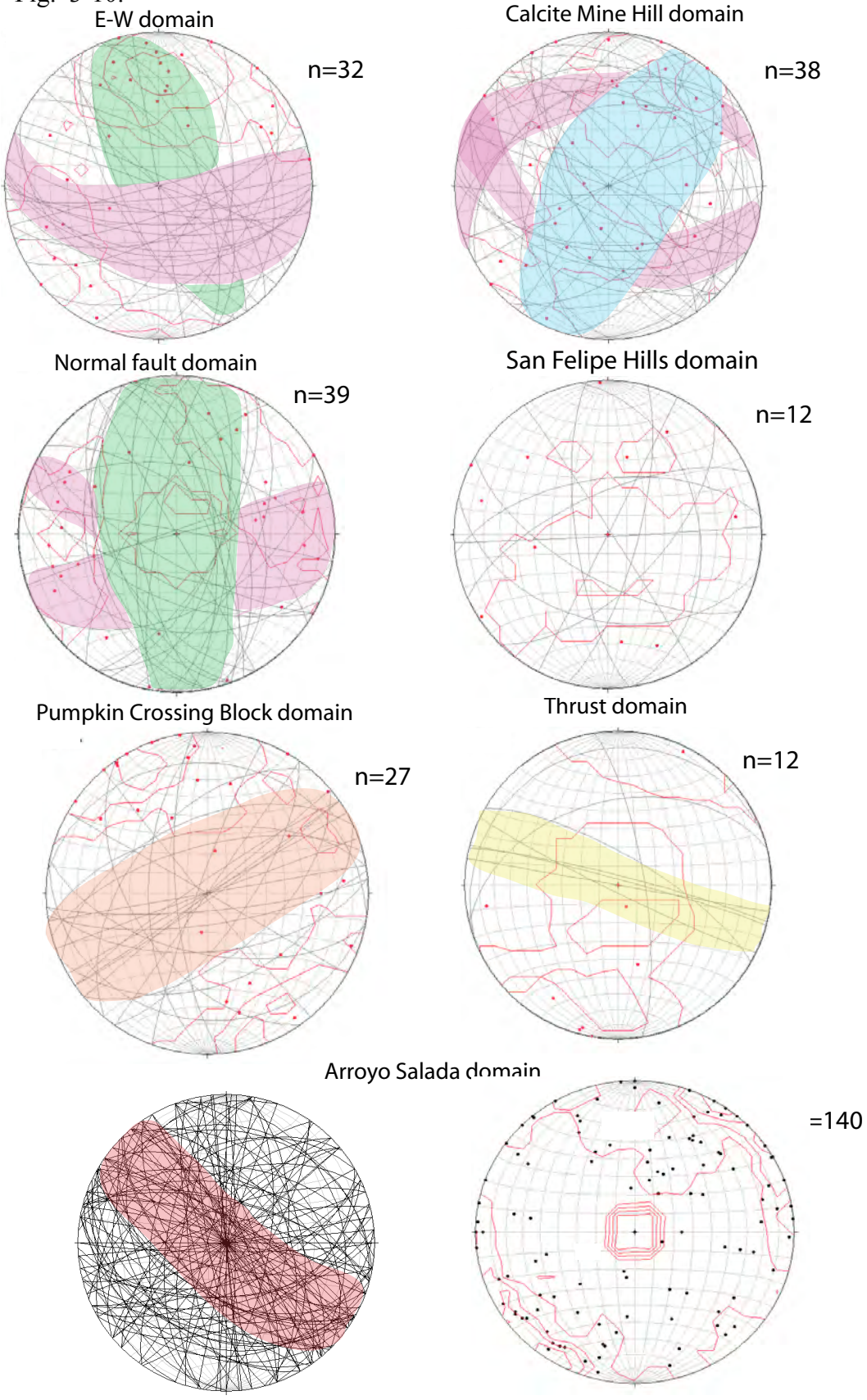
E-W domain
n=32
Calcite Mine Hill domain
n=38
Normal fault domain
n=39
San Felipe Hills domain
n=12
Pumpkin Crossing Block domain
n=27
Thrust domain
n=12
Arroyo Salada domain
=140

Fig. 3-10. Stereograms of fault planes within the interpreted fault domains of the Clark fault zone. Poles to planes (red dots) and Kamb contour intervals of 2 and significance level of 2 (red lines) are plotted. Data collected by the authors. Green shaded region is the north-south trending extensional faults that characterize the Normal fault domain and overlap the E-W domain. Purple indicates east-west striking dextral-oblique strike slip faults that characterizes the E-W domain and overlaps the Calcite Mine Hill and Normal fault domains. Red indicates the general orientation of the central Clark fault traces. Orange is the general orientation of the sinistral-oblique strike-slip faults that characterize the Pumpkin Crossing block fault domain, and the yellow indicates the reverse faults which characterize the thrust domain. Fault domains where too few data points were collected are not included.

The Santa Rosa fault domain is a 6-km long zone of dextral strike-slip faults that generally strikes 128°. The fault domain is 1-2-km wide and is defined by the 6 major fault traces of the southeastern part of the Santa Rosa segment of the Clark fault zone.

The Arroyo Salada fault domain is a 12-km long zone of dextral strike-slip faults striking ~129° and dipping nearly vertically or to the southwest at the surface. Although this domain is dominated the central traces of Arroyo Salada segment of Clark fault zone, many other faults with different orientations are present (Fig. 3-10). The northwest part of this domain is ~ 3-km wide and the domain increases its width to ~ 5 km to the southeast. The southeast boundary of this is the Pumpkin Crossing domain at the surface. The possibility of this fault zone continuing in the subsurface or as the offset Dump fault domain is discussed in further detail below.

The Calcite Mine Hill domain is dominated by east-northeast-striking sinistral-oblique faults that bend northward into the southeast part of the Santa Rosa Mountains (Fig. 3-7, 3-10). These faults intersect and terminate near the central trace of the Clark fault. A 4.5 km long fault in this domain crosses the central Clark fault and continues to the southwest. The sinistral strike-slip faults have some vertical slip (~ <0.2 km) near the northward bends (Plate 3). The Western Calcite Mine Hill fault is the largest fault within this domain (Plate 1).

The E-W domain overlaps with the Calcite Mine Hill domain and crosses the southern end of the Western Calcite Mine Hill fault (Fig. 3-10). This domain is dominated by east-west striking dextral strike-slip faults that splay off of the Central Clark fault zone near Smoke Tree Canyon. These faults have an oblique-down-dip component that collapsed the crest of the Graves Wash anticline (Weismeyer, 1968). The

eastern part of this domain overlaps the Normal fault domain in the northeast part of the study area. Near vertical east-west striking faults can be traced for up to 4 km without being cut by other faults. The Graves Wash fault is the major reverse fault in this domain described above. The normal overprinting of the reverse Graves Wash fault ties this fault into the E-W domain.

The Normal fault domain is characterized by multiple north-south-striking normal faults (Fig. 3-7, 3-10). These faults primarily dip towards the east and have normal east-side-down vertical displacements. The Four Palms Spring fault previously characterized above is the largest normal fault within this domain.

There are three fault domains in the southeast part of the field area that are dominated by northeast-southwest trending strike-slip faults with sinistral-oblique slip sense. The Pumpkin Crossing block fault domain is localized in an 8-km long crossing fault block, and is the structural boundary between the Arroyo Salada and San Felipe Hills fault segments of the Clark fault. Sinistral oblique strike-slip faults in the Pumpkin Crossing block fault domain have a southeast-side-down component of slip that repeats parts of the Borrego Formation (Plate 1). The NE sinistral fault domain maybe a continuation of the Pumpkin Crossing block fault domain that was displaced right laterally by faults in the Arroyo Salada and San Felipe Hills fault domains. The NE sinistral fault domain has at least 8 sinistral oblique faults spaced roughly 0.2 km apart. These faults strike north-northeast and could be continuations of the sinistral faults on the southwest side of the Clark fault zone. In the Short sinistral fault domain the faults are characterized by similar oriented east-northeast sinistral faults but their lengths are shorter (~2 km). The San Felipe Hills fault is a dextral strike-slip fault that serves as the

southwest boundary of all of the Pumpkin Crossing block and Short sinistral fault domains (Plate 1).

The Thrust domain is the area dominated by bedding parallel thrust faults in the southwest part of the study area. Gently dipping thrust faults on both sides of Palo Verde Wash have uplifted parts of the Borrego Formation up against Ocotillo Formation and also repeated the Borrego Formation. The area west of Palo Verde Wash requires additional mapping, but various sections of the north-dipping Borrego Formation are probably repeated by a series of bedding parallel faults with dip-slip components. This domain may be a restraining bend at the northwest end of the dextral San Felipe fault zone, and might link westward to the Coyote Creek fault zone (Fig. 3-2).

The San Felipe Hills fault domain is a structurally complex zone of en echelon, normal, and dextral strike-slip faults located in the southeast corner of the study area. Zones of highly faulted rocks where identifiable fault-bounded blocks range in size from kilometer to meter sizes are intermixed in a complex fault network (Fig. 3-11). Networks of smaller discontinuous faults are bounded by faults with larger displacements. Two major west-northwest trending complex en echelon fault zones are identified within this domain. These zones are 0.5 -1 km wide and $\geq$ 4 km long. A simple en echelon fault zone with strike-slip and down-slip components is located between the two complex en echelon zones. This en echelon array is characterized by 200-400 m-long fault traces that define an overall fault zone with a strike of 160° (Plate 1). This en echelon fault zone links to the south with the Powerline fault and continues ~ 10 km southeast of the study area to the Extra fault zone (Kirby, 2005). Steeply east-dipping normal faults dominate the western part of the en echelon fault zone. These faults repeat the top of the

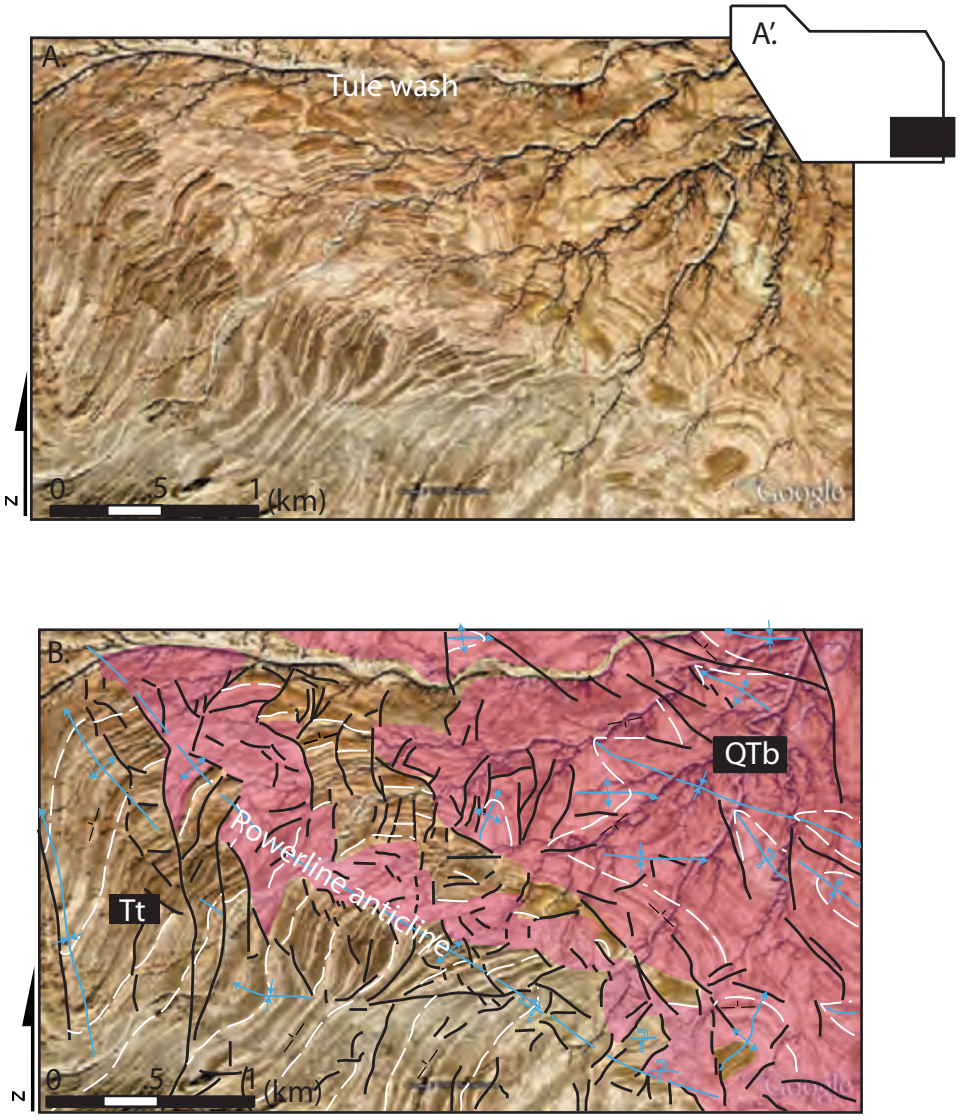

Fig. 3-11. (A) Google Earth images and geological interpretations of the complex en echelon fault zone in the San Felipe Hills fault domain. Dark beds are primarily sandstone and lighter beds are primarily mudstone of the Borrego Formation and transitional unit. (A') Black box is the location of the image relative to the study area. (B) Google Earth and geological interpretations. Black lines are fault traces, no slip indicators are represented due to complexity of each fault. Blue lines are fold axis with dip of beds and plunge of axis indicated by blue arrows, blue question marks are folds with unknown bedding dips. White dashed lines- bedding traces. Tt- transitional unit; QTb- Borrego Formation is highlighted in pink. Note the large northwest plunging Powerline anticline is defined by west, north and northeast dipping beds, and is clearly defined despite the complex faulting.

transitional unit three times and account for ~1 km of vertical offset (Plate 3, C-C'). In the southeast part of the en echelon fault zone north-striking faults have horizontal slickenlines and are dextral structures. A narrow zone of 0.1- to > 4-km long dextral strike-slip faults are located in the northeast part of this fault domain. The Dump fault is the largest of these dextral strike-slip faults. This part of the domain may be a southeast extension of the Arroyo Salada fault domain that has been offset by the Pumpkin Crossing block fault domain.

3.4. Evidence of Quaternary deformation

3.4.1. Quaternary deposits

A ubiquitous angular unconformity between the highly deformed Palm Spring Group and the nearly untilted pediment gravels suggests a decrease in tilting and folding prior to pedimentation, but without absolute ages of these pediment deposits our interpretations are limited. The oldest pediment gravels west of Salton City account for the highest topographic relief in the subbasin southeast of the Santa Rosa Mountains. Active incision and headword erosion by deep arroyos are exhuming much of the uplifted fault zone and pediment deposits that are up to 54 m above the active washes.

Other evidence of recent activity is observed in the fault scarps described below as well as the active folds and faults that are diverting drainages parallel to active faults and folds (Fig. 3-12). There is a major concave northeast bend of ~ 90° in the Arroyo Salada Wash just south of the Arroyo Salada Pediment, which is near the main trace of the Clark fault. Rattle Snake Canyon, and Palo Verde Canyon also have large bends where they intersect the central traces of the Clark fault. The Borrego syncline is actively diverting sediments of the Palo Verde Wash drainage system into its central axis as its

Fig. 3-12.

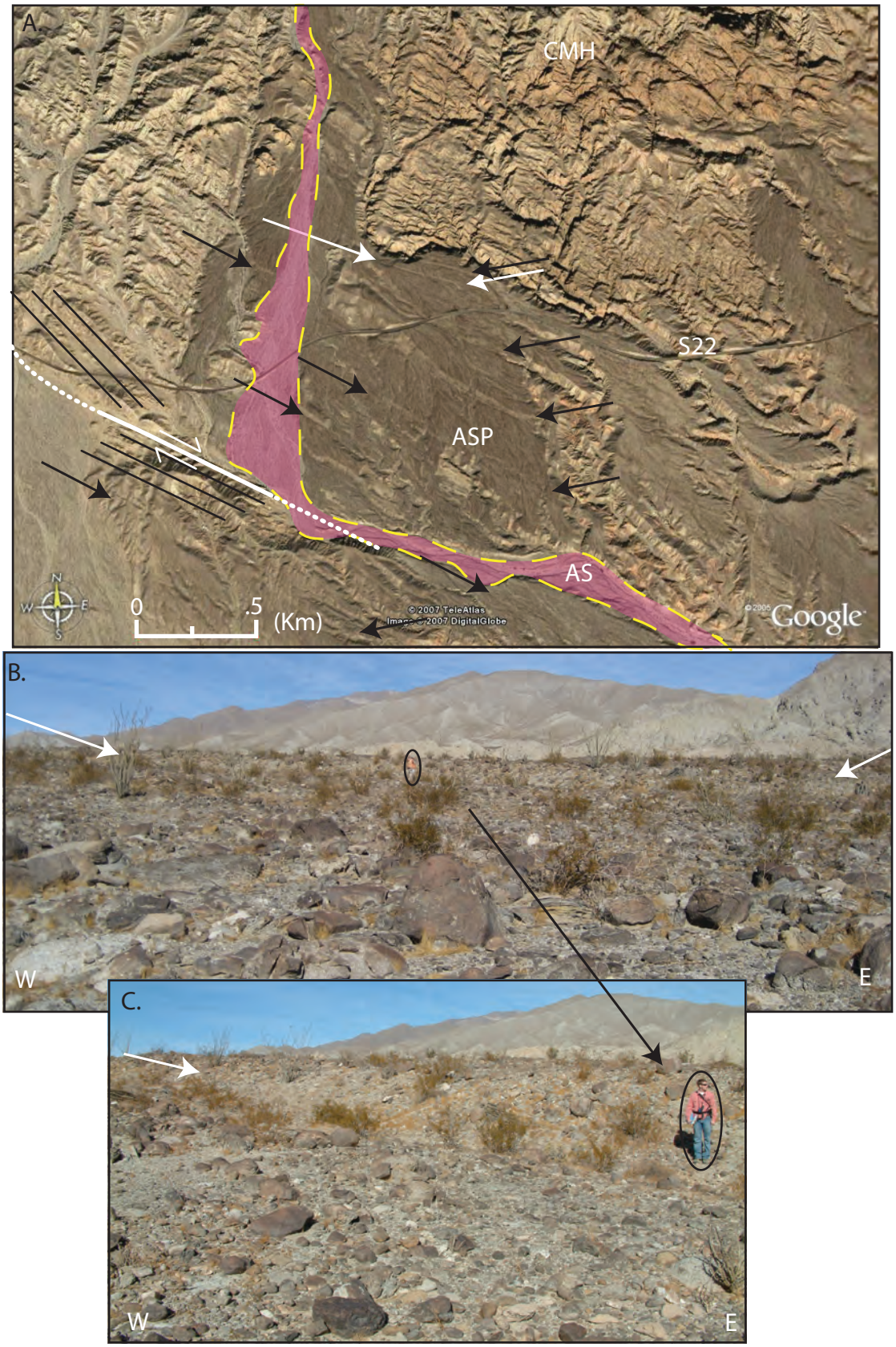
A.
CMH
S22
ASP
AS
0
.5
(Km)
© 2007 TeleAtlas
Image © 2007 DigitalGlobe
Google
B.
W
E
C.
W
E

Fig. 3-12. (A) Google Earth image of the region south of Calcite Mine Hill (CMH). The diverted Arroyo Salada (AS) Wash (pink and yellow) was diverted eastward by the fault of the central fault zone (white line) documented on Plate 1, and identified by the difference in strike of bedding indicated by the black lines. Fault scarps across the Pleistocene to Holocene Arroyo Salada pediment (ASP) are indicated by black arrows. Scarp faces create the lighter line with less desert erosion across the pediment surface. White line is a poorly exposed fault. White arrows indicate scarp in image B. C. (B) Photograph looking north across the pediment surface at a scarp face. Scarp face is indicated by white arrows, 5' 6''person for scale. Southern end of the Santa Rosa Mountains are in the background (C) Photograph looking north at the same scarp face as (B) 6' person is standing in a shallow channel created by flow diversions along the fault scarp (UTM 11S, 0580846, 3683101). White surface of scarp face is due to little or no desert varnished surface. Vertical offset of scarp is 1-2 meters. The down thrown surface in the foreground has a minor rollover component.

northeast and southwest limbs continue to be uplifted by oblique-dextral faults and folds (Fig. 3-13). Lute Ridge exposes and folds undifferentiated Quaternary deposits into an east-west trending anticline at its west end. The valley between the main trace of the Clark fault and northeast Borrego Badlands is a broad syncline of folded Quaternary deposits.

3.4.2. Fault scarps

Our mapping has identified approximately 25 km cumulative strike-length of fault scarps with vertical offsets of 1-3 m. Five to ten parallel fault scarps with mostly southwest down-dip-slip displacement cut middle Pleistocene to Holocene (?) pediment gravels in the central part of the Santa Rosa and Arroyo Salada fault domains. At least five scarps curve southward near the southeast end of the Santa Rosa segment at the Leon Pediment (Fig. 3-12). At least six north-south striking scarps with dominantly east-side-down displacements near the northeast part of the study area offset younger Pleistocene to Holocene (?) pediment gravels (Plate 1).

3.5. Microseismicity of the Southeast Clark Fault Zone

3.5.1. Two-dimensional analyses of earthquake epicenters

Microseismicity along the Clark fault zone within the northern San Felipe – Borrego subbasin grossly correlates with the structural deformation that we have mapped and analyzed at the surface (Belgarde and Janecke, 2006). A more precise analysis of these data has revealed that in general the zone of microseismicity in the Arroyo Salada and San Felipe Hills segments of the Clark fault is actually much narrower than the surface deformation related to the fault zone. Seismicity is concentrated in a ~ 5 km wide

Fig. 3-13.

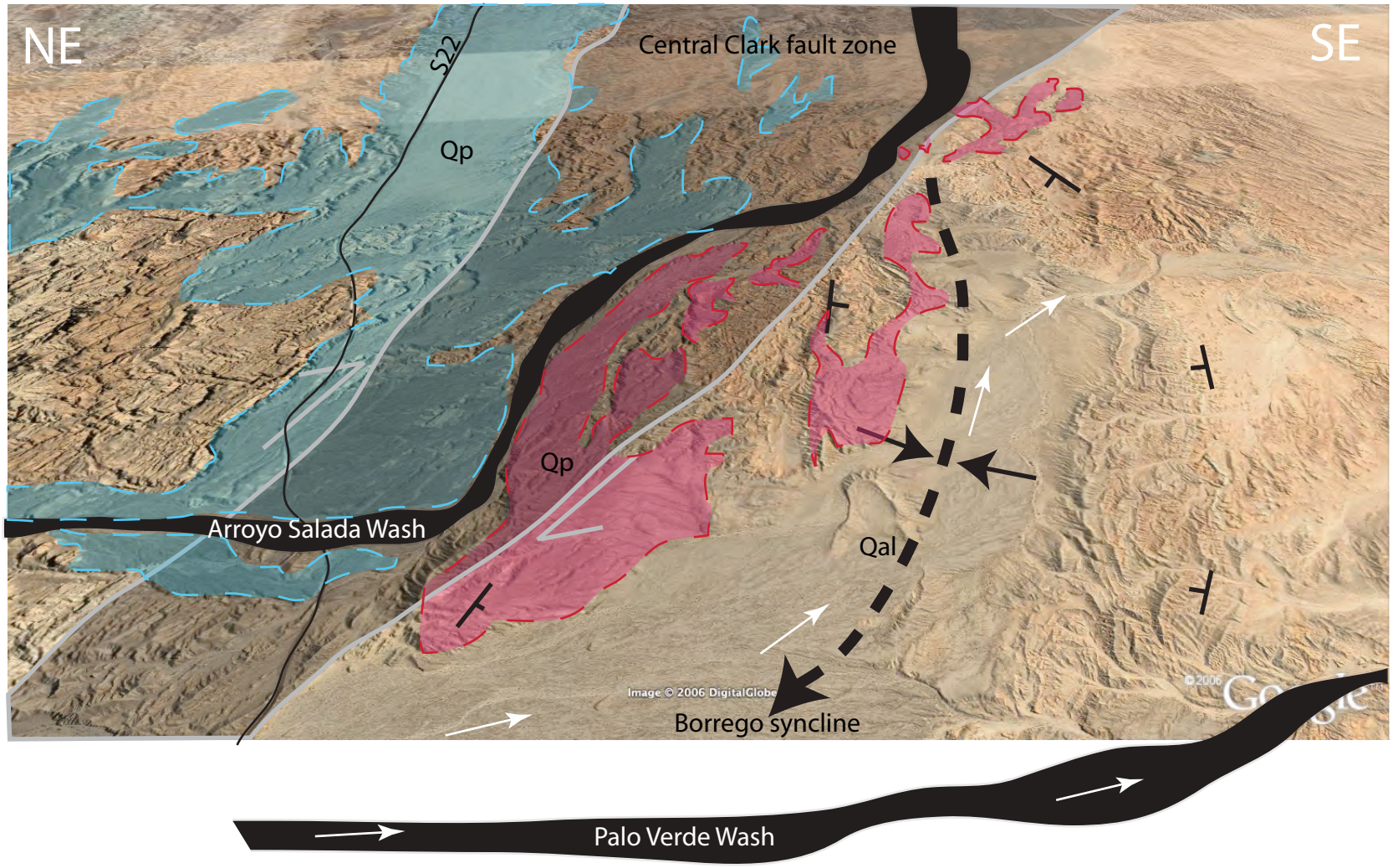
NE
SE
S22
Central Clark fault zone
Qp
Qp
Arroyo Salada Wash
Qal
Image © 2006 DigitalGlobe
Borrego syncline
Palo Verde Wash

Fig. 3-13. Google Earth image looking east-southeast down the axis of the Borrego syncline. ~ 9.1 km of the county road (S22) is shown in the figure for scale. The central Clark fault zone is darkened, and gray arrows indicate sense of slip. The black dashed line is the approximate axis of the Borrego syncline. Bedding orientations are shown. White arrows indicate direction of transport of the alluvial sediments (Qal). Pediments (Qp) and strath terraces northeast of the Clark fault is highlighted in blue and the southwest ones are red. Note that the undiverted Palo Verde Wash sediments are depicted by the black outline off the image, and the diverted Arroyo Salada Wash is also blackened.

zone between the southern edge of the Tower pediment and a northwest trending alignment 1-2 km southwest of Tule Wash whereas structural deformation related to the Clark fault persist from the Truckhaven fault in the north and the San Felipe Hills fault in the southwest, and is ~ 13 km wider (Fig. 3-14). Near the southeastern end of the Santa Rosa segment a ~ 2-km long zone of small earthquakes coincides with an active dextral-normal fault in the Arroyo Salada domain of the Clark fault. To the southeast of the Arroyo Salada segment the zone of seismicity widens abruptly to ~10 km (Fig. 3-15). Some earthquakes clearly nucleated on mapped faults whereas others show no relationship to the surface geology.

Areas lacking in microseismicity referred to herein as shadow zones exhibit as many faults and folds as parts of the fault zone with high levels of earthquake activity. One such shadow zone surrounds the 15-16 km long San Felipe Hills fault. Its microseismic shadow zone is ~ 5 km wide and is centered on the San Felipe Hills fault. Another shadow zone to the north of the Tower pediment surrounds the east-west striking Graves Wash fault and the north-south trending Four Palms Spring fault. There are multiple other faults and folds that deformed this area but produced few earthquakes in the last 25 years.

A northwest trending alignment of earthquakes at Lute Ridge persists southeast for ~ 22 km along the central trace of the Clark fault. We refer to this major alignment of earthquakes as the "Central alignment". The Central alignment has a gap northwest of the hypocenter of the 1954 M_w 6.4 Arroyo Salada earthquake but continues southeast as a concentration of earthquakes that broadens to a 1-2 km wide alignment that bends southward near the Pumpkin Crossing block (Fig. 3-15). At the northwest end of the

Fig. 3-14.

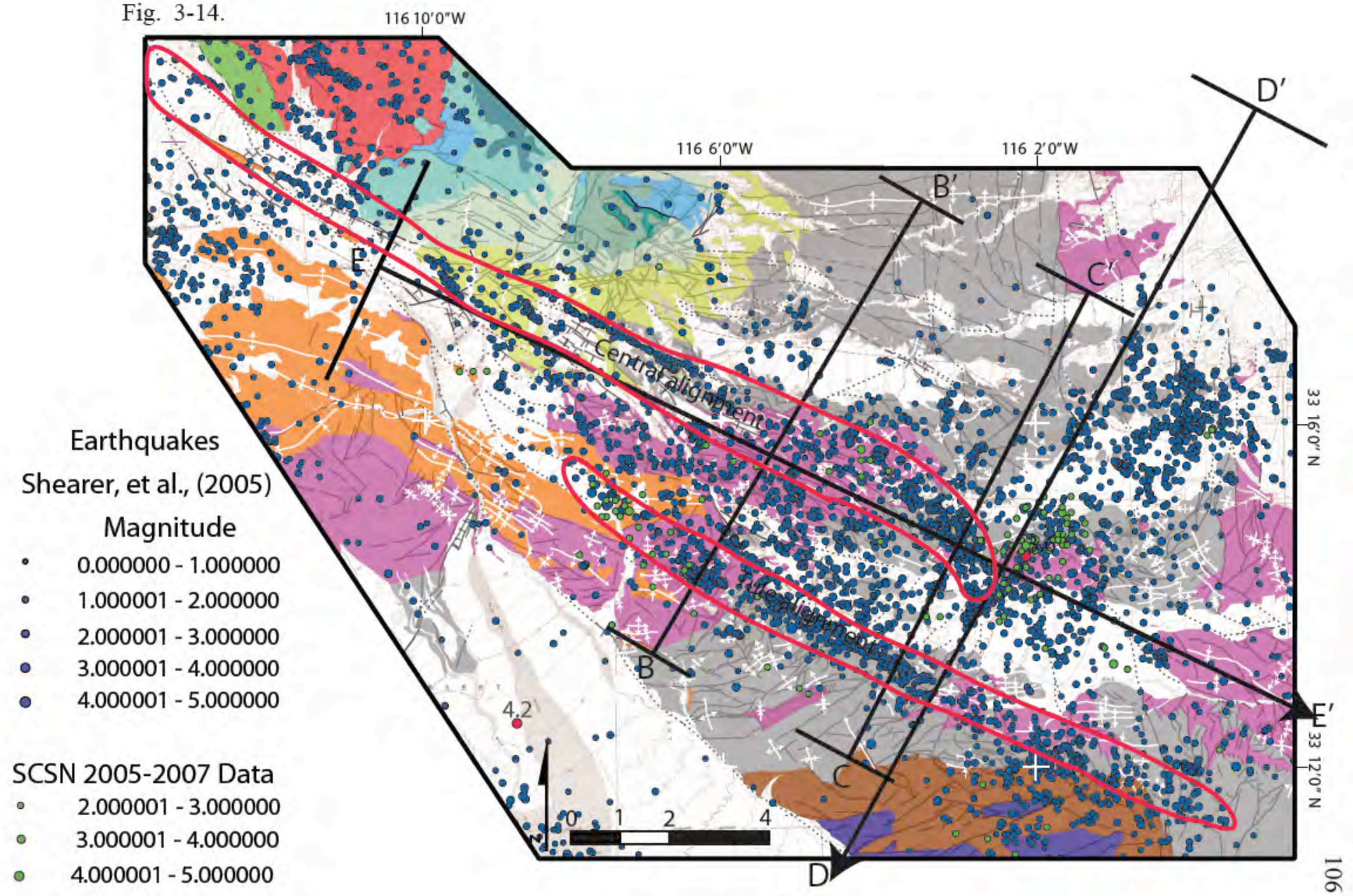
116 10′0″W
116 6′0″W
116 2′0″W
33 16′0″ N
33 12′0″ N
D′
B′
C′
E
E′
B
C
D
Central alignment
Eastern alignment
4.2
0
1
2
4
km
Earthquakes
Shearer, et al., (2005)
Magnitude
0.000000 - 1.000000
1.000001 - 2.000000
2.000001 - 3.000000
3.000001 - 4.000000
4.000001 - 5.000000
SCSN 2005-2007 Data
2.000001 - 3.000000
3.000001 - 4.000000
4.000001 - 5.000000

Fig. 3-14. Correlation between microseismicity and geology of the Clark fault zone. Refer to Plate 1 for the key to the geological map. Quaternary alluvium is white. Blue epicenters are from Shearer et al's (1982-2002) catalog and green epicenters (2002-2005) are from the SCSN catalog. The most recent M_L 4.2, and 3.6 earthquake epicenters are labeled and highlighted in red. Cross sections, B-B', C-C' and D-D' from figure 3-16 are shown. Refer to figure 3-15 for the location of A-A'. End bars on cross sections represent width of selection zone. Note the excellent correlation between faults and earthquakes along the Central alignment abut the clear mismatch between the Tule Wash alignment and mapped structures above it.

Fig. 3-15.

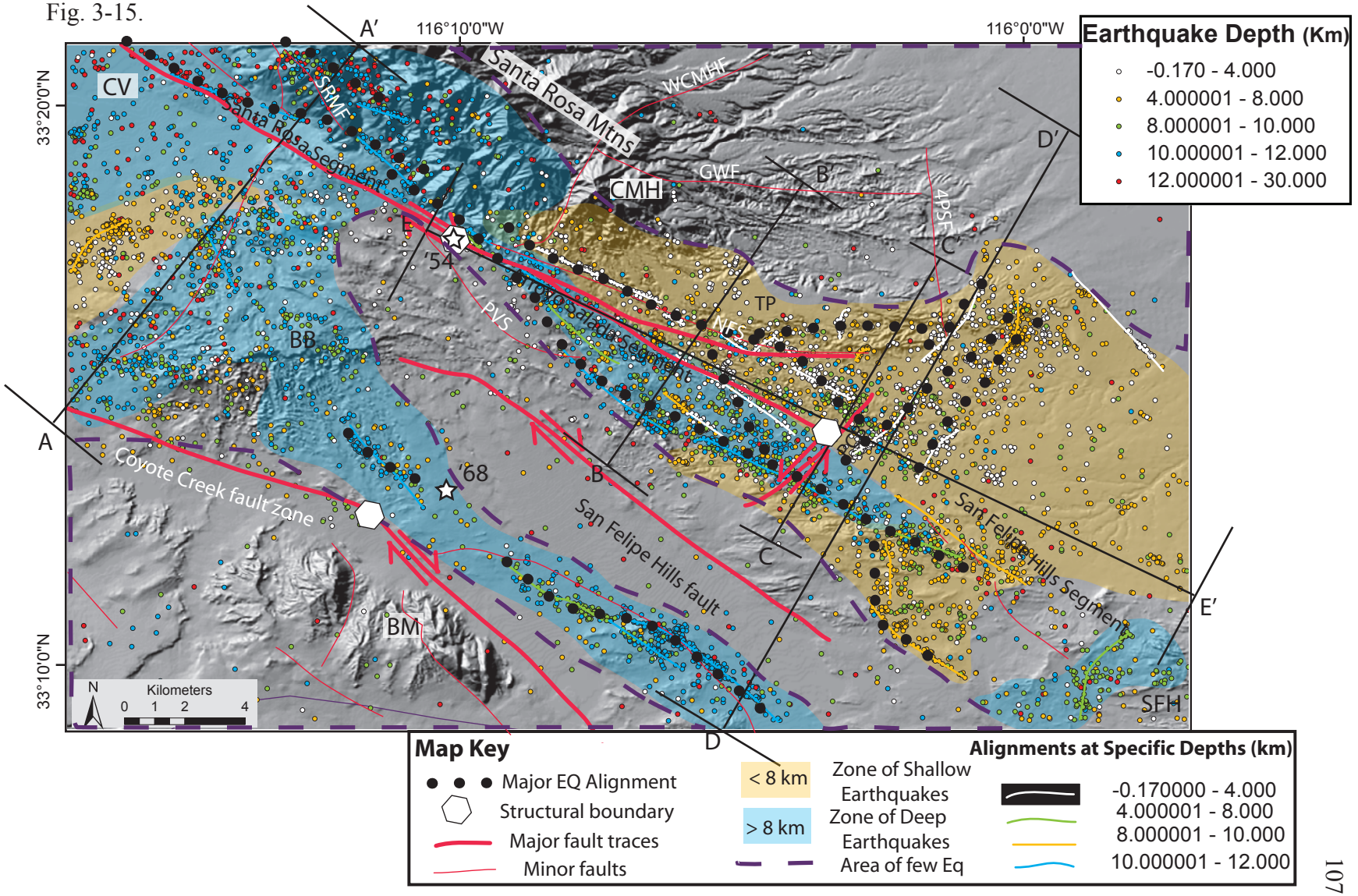
A′
116°10'0"W
116°0'0"W
33°20'0"N
33°10'0"N
CV
SRMF
Santa Rosa Segment
Santa Rosa Mtns
WCMHF
CMH
GWF
B′
D′
4PSF
C
'54
PVS
Thousand Palms Segment
TP
NFS
BB
A
B
'68
Coyote Creek fault zone
San Felipe Hills fault
C
San Felipe Hills Segment
E′
BM
SFH
D
N
Kilometers
0 1 2 4
Earthquake Depth (Km)
-0.170 - 4.000
4.000001 - 8.000
8.000001 - 10.000
10.000001 - 12.000
12.000001 - 30.000
Map Key
Major EQ Alignment
Structural boundary
Major fault traces
Minor faults
< 8 km
Zone of Shallow Earthquakes
> 8 km
Zone of Deep Earthquakes
Area of few Eq
Alignments at Specific Depths (km)
-0.170000 - 4.000
4.000001 - 8.000
8.000001 - 10.000
10.000001 - 12.000

Fig. 3-15. Interpretation of earthquake epicenters of the Clark and Coyote Creek fault zones. Dataset from Shearer et al (2005) plotted by depths. Boundaries between segments of the Clark fault and Coyote Creek fault are labeled. Shadow zones of regions with few earthquakes are outlined. Alignments at various depths are indicated. Notice the similar orientation of the deep seismogenic zones (blue) and the central trace of the Clark fault. Note the correlation between the earthquake alignments and fault traces. Cross sections from figure 3-16 are plotted. The epicenters of the 1954 and 1968 earthquakes are denoted by the white stars (Allen et al., 1968). BB- Borrego Badlands, BM - Borrego Mountain; CMH- Calcite Mine Hill; CV- Clark Valley; 4PSF- Four Palms Spring fault; GWF- Graves Wash fault; NFS - North Fork Splay; PVS- Palo Verde splay; PCB- Pumpkin Crossing block; SFH- San Felipe Hills; SRMF - Santa Rosa Mountain fault; SP- Squaw Peak; TP- Tower pediment; WCMHF - Western Calcite Mine Hill fault. Fault traces modified from Kirby, 2005; Steely, 2006; and this study.

Arroyo Salada segment a major alignment, termed the "Tule alignment," branches south from the Central alignment and lies ~ 2 km northeast of the San Felipe Hills fault trace. The Tule alignment is produced by earthquakes that are between 8-12 km deep (Fig. 3-15). There is no through-going fault that correlates to this deep alignment at the surface and many mapped faults clearly cross the deep alignment. The southern end of the Tule alignment continues past the Pumpkin Crossing block for 4 km where it dies out in the northern San Felipe Hills segment. Another major splay off the Central alignment follows the southern edge of the Tower pediment and dies out or is truncated by a northeast-southwest alignment of earthquakes associated with the Pumpkin Crossing block fault domain. There is a ~ 4-km long alignment of earthquakes trending 160° between the Central and the Tule alignments.

There are two major alignments of earthquakes trending northeast-southwest that correlate with the Pumpkin Crossing block. These are shallow alignments made of earthquakes between 0 and 8 kilometer depths. These major alignments are 8-10 km-long and have northeast trending minor alignments associated to them. There is a large cluster of earthquakes where the central alignment and the westernmost northeast-southwest oriented alignment intersect. Beyond this zone of crossing alignments to the southeast the seismic density greatly decreases.

3.5.2. Three dimensional analyses of earthquake hypocenters

Most of the earthquake alignments described above define planar features in three-dimensions. Cross sections show defined alignments of planar features at depth (Fig. 3-16). These cross sections reveal a zone between 5 and 10 km deep where very few earthquakes occur. This vertical patter may represent a weak decollement layer in the

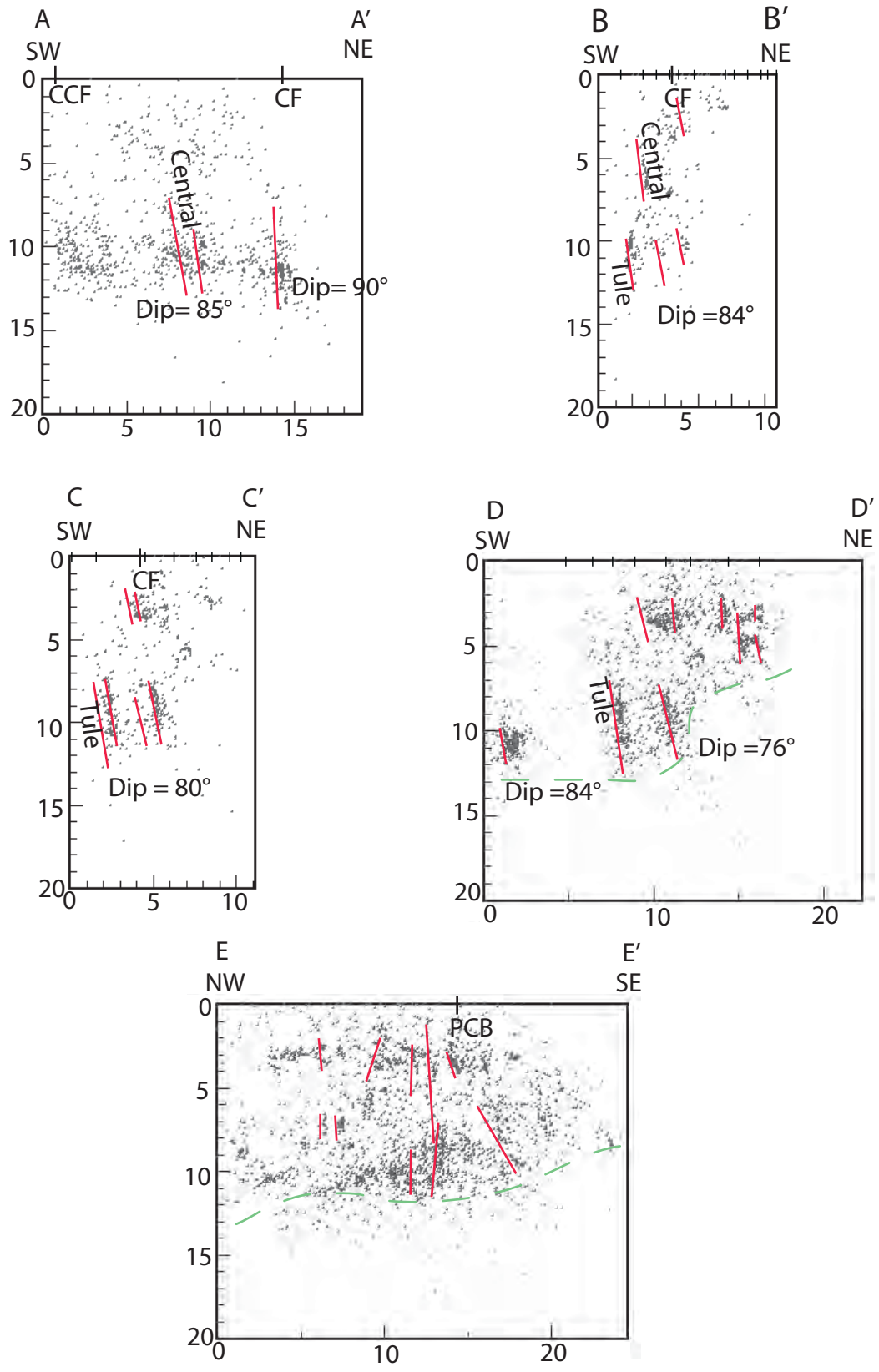
A
SW
A′
NE
CCF
CF
Central
Dip= 85°
Dip= 90°
B
SW
B′
NE
CF
Central
Tule
Dip =84°
C
SW
C′
NE
CF
Tule
Dip = 80°
D
SW
D′
NE
Tule
Dip =76°
Dip =84°
E
NW
E′
SE
PCB

Fig. 3-16. Cross sections of microseismicity along the Clark fault zone. Red lines are parallel to earthquake alignments, green denotes the base of seismogenic zone, Black indicates where fault traces from the geological map intersect the central trace of each cross section, and major fault traces are labeled, CF- Clark fault; CCF- Coyote Creek fault; PCB - Pumpkin Crossing block. Widths of the selection zones for each cross section are, A-A': 5 km, B-B': 2 km, C-C': 2 km, D-D': 3.5 km, E-E' 5.5 km.

subsurface. They also show major planar features that consistently dip steeply towards the northeast. Alignments of earthquakes are more defined when the hypocenters are subdivided into five different depth levels (Fig. 3-15). A deep zone of earthquakes > 8 km wide located in the southeastern Santa Rosa Mountians continues southeast into the San Felipe-Borrego subbasin along the Central alignment. These clearly formed in the Santa Rosa and Arroyo Salada fault domains at depth and are concentrated in a 2-km wide zone. Another northwest trending zone of deeper alignments is located in the eastern Borrego Badlands narrows from ~10 km wide to 2 km wide towards Squaw Peak. This is the deep expression of the Squaw Peak fault (Steely, 2006). A major zone of shallow earthquakes persists northeast and southwest of the Clark fault's central trace.

The Tule and Central alignments are the two major alignments within the deep zone of microseismicity. Each of these alignments have earthquakes concentrated between 7-12 km depth. The central alignment in particular is made of especially well defined short alignments that are at depths greater than 8 km (Fig. 3-15). The deepest alignments are beneath the Santa Rosa Mountains.

Many shallow alignments are observed with the study area. There is a north-northwest trending alignment of hypocenters < 4 km deep just south of Calcite Mine Hill that correlates to an active dextral-oblique fault with scarps formed in Pleistocene to Holocene (?) pediment deposits (Fig. 3-12, 3-16, and Plate 1). Shallow earthquake alignments tend to have the same spatial distributions and trends as scarps documented in the study area (Fig. 3-15).

The earthquakes abruptly decrease in maximum depth southeastward at the Pumpkin Crossing block from a maximum depth of ~ 14 km in the northwest to a

maximum depth of <10 km in the southeast (Fig. 3-16, E-E'). In cross sections perpendicular to the Clark fault earthquake alignments dip consistently to the northeast between 85-76° (Fig. 3-16). Near the northwest part the study area, across the Santa Rosa Segment, 3 well-defined alignments of earthquakes are documented at upper to mid crustal levels (8 -12 km) that dip between 85 - 90° to the north-north-northeast (Fig. 3-16, A-A'). The surface faults near this area dip consistently towards the southwest, and however we suspect that the northeast dipping fault planes at depth curve upward and are expressed by nearly vertical to southwestward dipping faults at the surface (Plate 3, A-A').

The central part of the Arroyo Salada segment contains three en echelon alignments in cross section view that dip ~84° to the northeast. The southwesternmost alignment is below 10 km depth and is part of the Tule alignment (Fig. 3-16, B-B'). The southeasternmost part of the Arroyo Salada segment has six well defined alignments at two crustal levels. There are two alignments that dip 80-86° above 4 km depth and four major alignments with similar dips below 7 km. The total width of the cluster in cross section view is ~ 8 km wide. This is an increase in width of ~ 4 km relative to the seismic width of the central part of the Arroyo Salada segment (Fig. 3-16, B-B', C-C').

The seismic cross section parallel to the Pumpkin Crossing block reveals multiple small alignments above 5 km depth and 3 larger alignments below 7 km. A zone of little seismicity lies between these depths. There are no deep alignments on the northeast side of the central traces of the Arroyo Salada fault domain. This cross section continues southeast to Squaw Peak where a well defined alignment persists below 10 km on the Squaw Peak fault.

3.5.3. Recent earthquake activity

Since the beginning of this study in 2005 there have been a number of earthquakes with magnitudes greater than 2 in the Clark fault zone. A M_L 4.2 earthquake occurred on February 9, 2007 (UTC) 12 km under Palo Verde wash in the southwest part of the study area (Southern California Seismic Network event Id 10230869)(Fig. 3-14). This earthquake occurred at the edge of the shadow zone surrounding the San Felipe Hills fault, but is more likely related to a northern extension of the dextral strike-slip fault documented south of the study area near Squaw Peak (Kirby, 2005; Steely, 2006).

There is a prominent cluster of recent earthquakes that began with a M_L 3.6 on July 8, 2006 (UTC) near the Pumpkin Crossing block (Southern California Seismic Network event Id 10200841) (Fig. 3-14). This cluster of earthquakes trends roughly 30°. The northern end of this alignment coincides with the intersection of the Dump fault and the longest sinistral fault zone of the Pumpkin Crossing block (Fig. 3-14).

4. Discussion

4.1. Continuation of the Clark Fault Zone

The southeast end of the Clark fault is traditionally mapped near Smoke Tree Canyon at the northwest end of the Arroyo Salada segment (Dibblee, 1954, 1984; Hoover, 1965; Sharp, 1967; Jennings, 1977). Our work shows that this area is a segmentation boundary instead of an endpoint. Geological and microseismic evidence clearly shows that the Clark fault continues an additional ~ 25-30 km southeast from this boundary into two additional fault segments. The detailed observations made in this study and Kirby's (2005) detailed work to the southeast we document that active deformation related to the Clark fault continues southeast to the crossing Extra fault zone.

The Arroyo Salada segment is ~ 11-12 km long extending southeast to the ~ 3-4 km wide Pumpkin Crossing block. Beyond the Pumpkin Crossing block the San Felipe Hills segment extends the Clark fault another 12-13 km to the southeast.

4.1.1. Geological Evidence

The 14.5-18 km of right separation on the Santa Rosa segment northwest of this study (Sharp, 1967; Janecke et al., 2005) is expressed by a highly complex zone of deformation within the sedimentary rocks of the northern San-Felipe Borrego subbasin. Prior to this study little has been done to document how strain is transferred through the area. We identified 6 fold and 10 fault domains that accommodate the dextral deformation in the Arroyo Salada and San Felipe Hills segments. In addition to the central fault traces of the Arroyo Salada and Santa Rosa fault domains there are at least 9 subsidiary faults and 4 subsidiary folds that account for much of the strain in this 2-18 km wide zone of deformation (Table 3-1). The central fault traces in the Arroyo Salada domain of the Arroyo Salada segment are the southeast continuation of the fault traces in Santa Rosa domain of the Santa Rosa segment. These 2 domains are a zone of at least 10 oblique-dextral strike-slip faults that strike 125-129°. The Arroyo Salada fault domain continues approximately 12 km to the southeast where it intersects with the Pumpkin Crossing block. This crossing fault block (Pumpkin Crossing block) is a ~ 3 km wide structural boundary between the Arroyo Salada and San Felipe Hills segments. Beyond this structural boundary major dextral strike-slip faults (Dump, Powerline, and Sand Dunes faults) and complex en echelon fault arrays dominate the central 5-6 km of the San Felipe Hills segment southeast of any previously identified segments of the Clark fault (Kirby, 2005; this study). The intense folding strain documented by Feragen (1986),

Wells (1987), Reitz (1977), Heitman (2002), Lilly (2003), and Kirby (2005) (up to 30% shortening) formed in the Clark fault zone as the southeast end of the San Felipe Hills segment interacted with the crossing sinistral Extra fault zone (Fig. 3-2).

4.1.2. Microseismic Evidence

Analysis of the highly active zone of microseismicity in the central part of the study area strengthens our structural interpretation of the Clark fault. Multiple alignments of earthquakes coincide with mapped faults and help us to better locate active strands of the Clark fault (Fig. 3-14). There is a southeastward decrease in microseismic activity (Fig. 3-14), but we suggest that this is due to strain differences across the Pumpkin Crossing block and not due to the termination of the Clark fault zone. In the San Felipe Hills segment most earthquakes are < 8 km deep and are distributed across a much wider zone perpendicular to the central traces of the fault zone (Fig. 3-15).

4.2. Structural Geometry of the Southeast Part of the Clark fault

4.2.1. Structural models of strike-slip faults

The structural geometries of this fault zone can be explained by a combination of strain partitioning, wrench fault models, and complex fault geometries that build upon Andersonian rock mechanics. Evidence that we have documented within the northern San Felipe-Borrego subbasin that supports the wrench fault model and the strain partitioning model as well as more complex models is presented below.

Some folds and most of the faults interpreted in the study area are oriented in accordance to the predicted orientations of the wrench fault model for a horizontal maximum compressive stress oriented ~ 350° and 170° (Wilcox et al., 1973; Townend

and Zoback, 2004) (Fig. 3-3A.). Major components of north-south shortening are represented by east-west striking thrust faults and folds. The east end of the North Fork splay is a good example of an east-west striking thrust fault. There are many other east-west striking faults that have thrust components throughout the study area (Plate 1). East-west trending folds account for the main components of shortening in the Tule Wash, the North Fork, and the Graves Wash fold domains (Fig. 3-6, Table 3-1). The wrench fault model also predicts extensional features that are oriented parallel to the maximum compressive stress. We documented more than 20 large north-south striking normal faults like the Four Palms Spring fault that show general east-west extension ~ 10-20° clockwise from the predicted orientation of 350°. The major strike-slip faults are oriented at angle 10-20° counterclockwise or clockwise than the wrench fault model would predict but sinistral faults are generally oriented northeast-southwest and dextral faults are oriented northwest –southeast as expected. Many of the strike-slip faults have oblique-slip components that probably explain some of the differences in the geometries observed relative to the predictive wrench fault model.

The study area contains many structures that are oriented sub parallel to one another yet have very different kinematics, and this may be explained by a strain partitioning model. In the southeast part of the study area there are multiple instances where folds and strike-slip faults are parallel to one another. This could be explained by separating the strain field into a pure strike-slip component and a pure shortening component (Fig. 3-3B). The most prominent example of this behavior is the near parallelism of the Borrego syncline and the central traces of the Arroyo Salada fault domain. These structures differ in orientation by only 10° yet the syncline appears to be

dominated by pure northeast-southwest shortening and the fault is primarily a dextral strike-slip fault (Table 3-1). This association is very common in the area and many other examples of northeast or northwest trending folds with adjacent northeast or northwest-striking strike-slip fault have been discovered throughout the study area (Plate 1).

The Borrego syncline could also be explained by geometric heterogeneities in the fault plane. Shortening can be produced by bends in the fault plane at depth. Major fault bends that occur between the southwest dipping surface traces and the northeast dipping faults at depth may produce enough shortening along the Clark fault to produce the Borrego syncline without strain partitioning. Although this fault bend fold model and strain partitioning could explain the Borrego syncline we cannot presently rule out any alternative.

4.2.2. Simplified structural model of the southeast Clark fault

The Clark fault continues through the northern San Felipe Hills subbasin as a southeast widening zone of deformation (Fig. 3-17). Strain is partially obstructed by a Pumpkin Crossing block in the shallow crust, but continues further to the southeast where it terminates at the Extra fault zone (Kirby, 2005). We observe mutual interference of many of the major structures throughout the study area. The deformation within this area is dominated by wrench faults, but complexities in local structural geometries create anomalous orientations of folds and faults at all scales throughout the study area.

The central traces of the Clark fault enters into the sedimentary rocks of the basin striking parallel to bedding planes. Once the major strike-slip fault zone enters into this zone of bedding-strike parallel deformation, it is impossible to find offset markers to

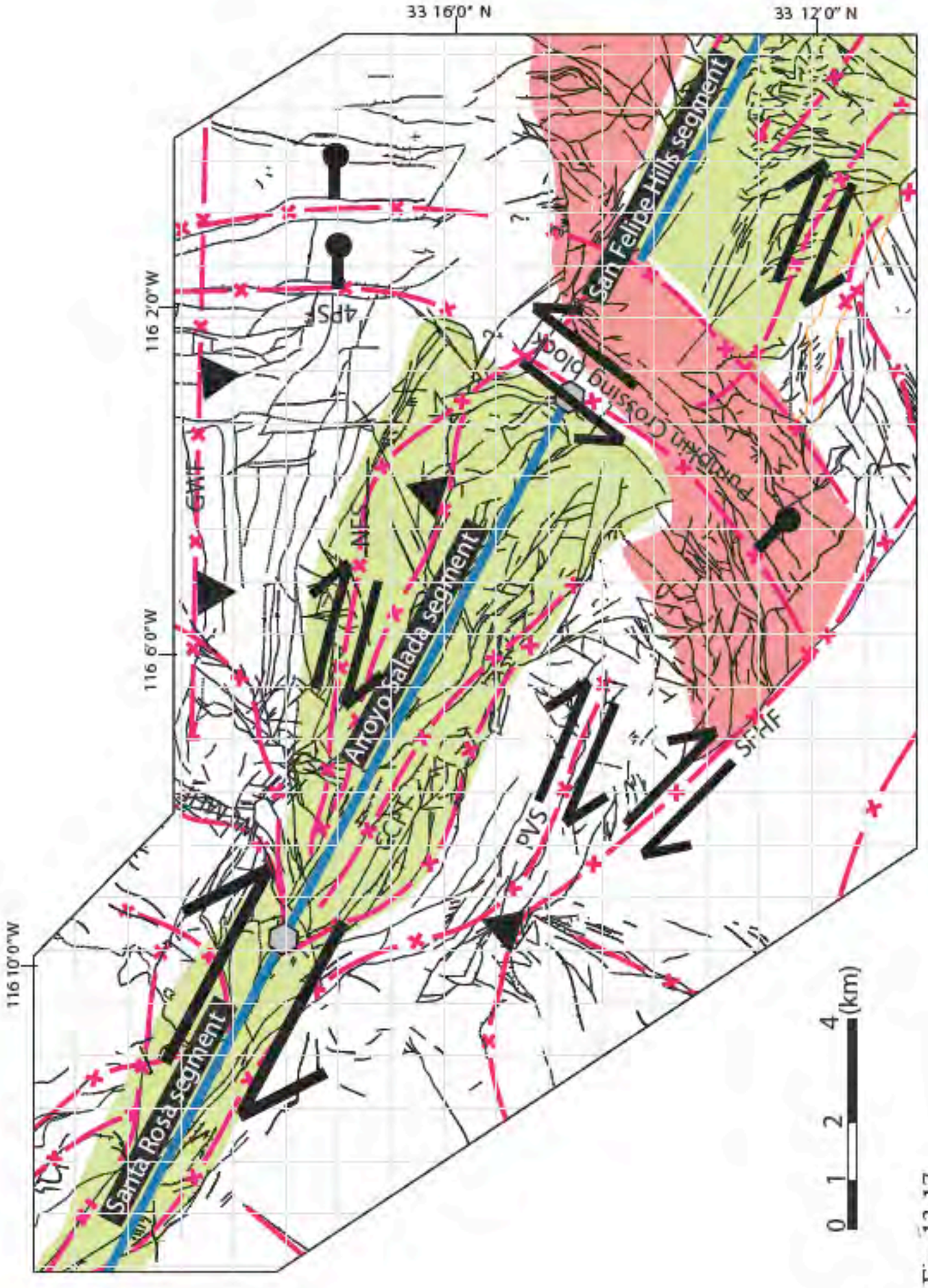
33 16'0" N
33 12'0" N
116 2'0"W
116 6'0"W
116 10'0"W
4PS
GMF
NF
San Felipe Hills segment
Powerline Crossing block
Arroyo Salada segment
SCF
PVS
SJHF
Santa Rosa segment
0
1
2
4
(km)

Fig. 13-17.

Fig. 3-17. Simplified structural model of the faults within the study area. Major fault strands are pink. Black indicates sense of slip. The Santa Rosa Arroyo Salada and San Felipe Hills fault domains are shaded green. The Pumpkin Crossing block and NE sinistral fault domains are shaded orange. CASFT: Central Arroyo Salada fault traces; 4PSF- Four Palms Spring fault; GWF- Graves Wash Fault; NFS- North Fork splay; PVS - Palo Verde splay; SFHF- San Felipe Hills fault; WCMHF- Western Calcite Mine Hill fault. Solid blue line is the main trace of the Clark fault in the Santa Rosa, Arroyo Salada and San Felipe Hills segments.

estimate slip across the fault zone. Calculating the separation along the 100's of small faults and folds that contain centimeters to 100's of meters of offset is beyond the scope of this project and probably impossible, but we suspect that a major part of strain (? 60% - 80% ?) is represented in this distributed off-fault deformation. We have not ruled out the possibility of localized block rotation and can only speculate that shear of fault blocks has occurred between many of the major fault splays. Such block rotation may explain the many faults that are clockwise of their predicted orientations. We must also take into account a small southwest-down component of slip across the Santa Rosa segment of the Clark fault. This decreases the amount of observable dextral slip. Because of these structural difficulties and incomplete understanding of local stratigraphy it is difficult to provide meaningful estimates of slip across the faults of the Arroyo Salada and northern San Felipe Hills segments.

The simpler linear traces of the Clark fault in the Peninsular Ranges changes into a wide complex zone of deformation in the San Felipe – Borrego subbasin (Dibblee, 1954; this study). The lithological differences between the sedimentary rocks of the San Felipe – Borrego subbasin and the crystalline rocks of the Peninsular Ranges are partially responsible for this change in deformation. In the basin mud-rich rocks within the sedimentary rocks also change the style of deformation (Fig. 3-18; Chapter 4). This is documented at the map scale by a huge increase in the density of folds in rocks that are rich in finer-grained material relative to crystalline and coarser rocks that at most have a few broad folds. At the outcrop scale mud-rich sedimentary rocks deform ductily around faulted coarse-grained blocks in damage zones along individual fault splays.

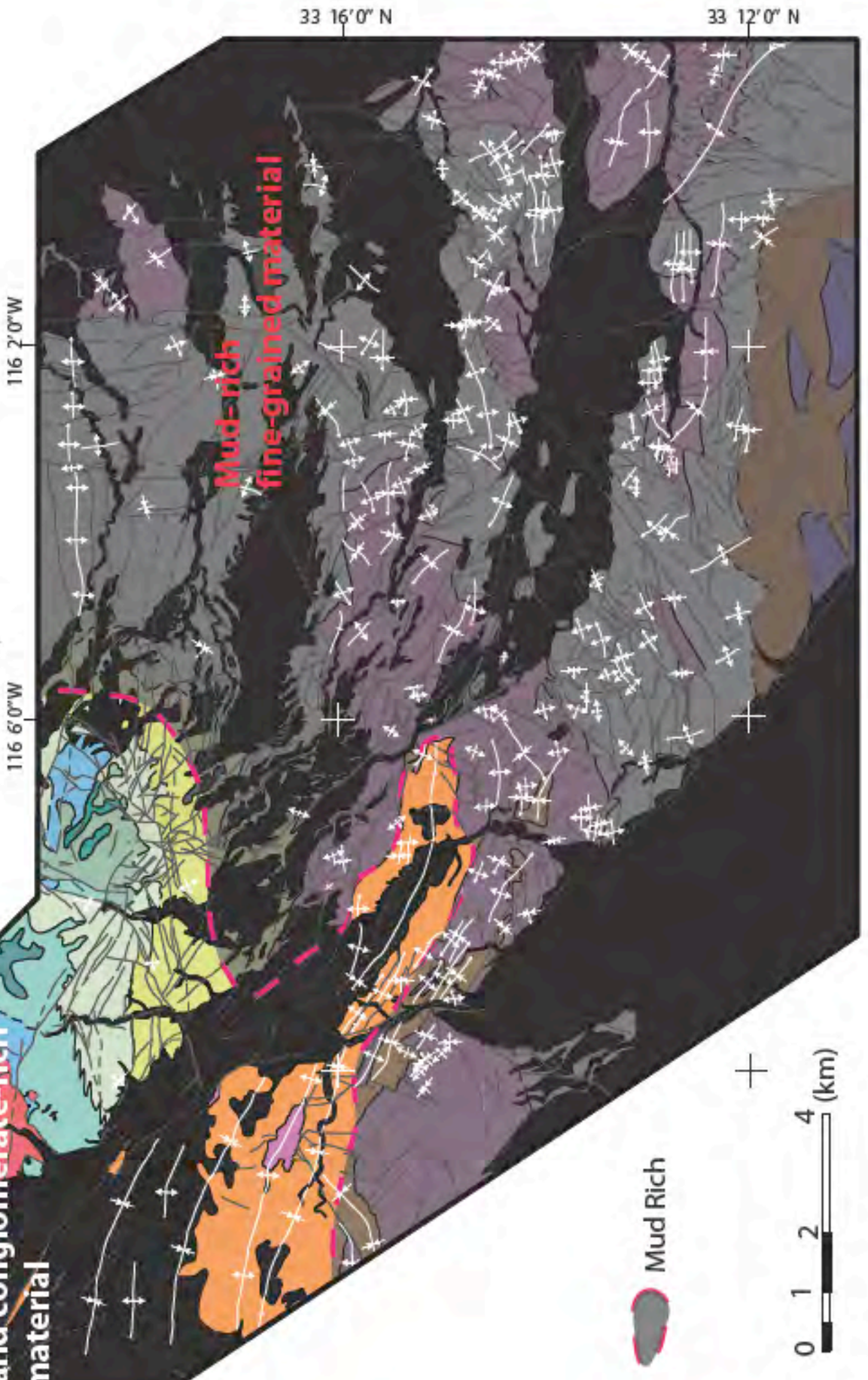
33 16′0″ N
33 12′0″ N
116 2′0″W
116 6′0″W
116 10′0″W
Mud-rich fine-grained material
Crystalline rocks and conglomerate-rich material
σ_1
Mud Rich
0 1 2 4 (km)

Fig. 4-20.

Fig. 3-18. Comparison of the rock types and structural patterns of the Clark fault. Refer to Plate Map for the key to the geological map in the background. Deposits younger than the Ocotillo Formation are blacked out. The mud-rich sedimentary rocks make up the grayed region. Notice the dramatic increase in the number and length of folds relative to the crystalline rocks (red, green) and the coarse grained sandstone to conglomerates (shades of blue and green, orange).

The major structures adjacent to the Clark fault provide evidence that structural geometries also control the orientation of faults and folds. The Extra fault zone to the southeast is obstructing the southeast continuation of the Clark fault zone. The increase in the width of the Clark-fault-related deformation may be partly caused by this obstruction as well as by the smaller Pumpkin Crossing block at the southeast end of the Arroyo Salada segment. The deformation adjacent to the Coyote Creek fault is narrower even though the fault is slightly younger and has less separation (Janecke, and Dorsey unpublished mapping). We suggest that some of the differences in damage adjacent to the Clark and Coyote Creek faults are due to the Crossing Pumpkin block and Extra fault zone (Fig. 3-2).

4.2.3. Linkages with adjacent structures

The Coyote Creek fault zone branches southward from the Horse Canyon segment of the Clark fault. Major fault connections between the Coyote Creek fault and the Clark fault southeast of this point have been previously document in areas such as the Coyote Mountains, Borrego Badlands, and San Felipe Hills (Bartholomew, 1970; Sharp, 1975; Dorsey, 2002; Janecke et al., 2005; Lutz et al., 2006; Kirby et al., 2007). The San Felipe Hills fault is possibly another major linkage structure between these two faults. Strain from the Clark fault is clearly distributed onto the San Felipe Hills fault by the complex network of northeast-southwest and east-west strike-slip faults in the northwest San Felipe Hills and by dextral faults along Palo Verde Wash. The San Felipe Hills fault may become a northward dipping thrust fault to the west of Palo Verde Wash and continue west into an unproven speculative contraction link to the Coyote Creek fault.

The San Felipe Hills fault has so many linkages with the adjacent faults that it can't be confidently included in either the Clark or Coyote Creek faults.

Our mapping also shows that the Buck Ridge fault zone merges southeastward with the Santa Rosa segment of the Clark fault in the northwestern part of the study area. This interaction clarifies previous interpretations of the southern extent of the Buck Ridge fault zone where Sharp (1967) incorrectly shortened Dibblee's (1954) originally interpreted Buck Ridge fault. The map shows that the Santa Rosa fault in the northwest part of the study area links strain from the Buck Ridge fault to the three southern segments of the Clark fault.

4.3. Seismic effects and associated hazards

4.3.1 Earthquake hazards

Fault scarps, active folds, and diverted drainages and the abundant microseismicity provide conclusive evidence that this is a highly active fault zone. As the science of earthquake predictions moves forward our structural characterization of this area may help us to better understand similar fault zones that are actively deforming sedimentary basins beneath large metropolitan areas. Our structural investigations (Kirby, 2005; Kirby et al., 2007; this study) have extended the length of the active Clark fault trace at least ~ 15 km southeast of any previously identified termination point by first characterizing the structural deformation, and then correlating those structures with microseismic alignments. One inference from our investigation may be an increase in the magnitude of a potential earthquake because the Clark fault is longer (seismic moment = fault area $*$ slip $*$ rigidity). Although very few people will be affected by a large earthquake along the Clark fault the structural interpretations in this study may be used as

an analogy for other more densely populated basins cut by poorly understood strike-slip faults. Similar interpretations of microseismicity along faults that are poorly exposed or have limited access may prove to be a good way to fill in crucial voids in the geological mapping of metropolitan areas.

4.3.2. Implications for Paleoseismology

The detailed structural investigation has revealed a very broad deformation zone in the southern two segments of the Clark fault. Multiple fault splays within these two segments accommodate various proportions of the total dextral strain. We see no practical way to estimate slip-rates in a deformation zone as wide as the Clark fault using paleoseismic techniques. We also suggest that paleoseismic studies in other areas where the extent of the fault zone is poorly understood may produce slip-rates that are too low if they also have distributed fault zones as well. Unrepresentative lower slip-rates along poorly understood fault zones understate the actual seismic hazard, and pose a greater risk to the surrounding communities. Complete structural analysis of fault zones in metropolitan areas must be conducted in order to accurately determine the percentage of the slip-rate being characterized by a paleoseismology study of a single fault. The Imperial fault zone, in the middle of the Salton Trough, may be such an example (Thomas and Rockwell, 1996; Shearer, 2002). It should be slipping at nearly the plate rate but paleoseismology reveals less than half of that (Thomas and Rockwell, 1996). A microseismic and structural investigation of this fault zone similar to our investigation may explain this discrepancy.

4.3.3. Structural vs. seismic segmentation

Seismic segment boundaries are most commonly terminations or initiation points of earthquake ruptures (Sanders, 1989; Shearer, 2002). Structural segment boundaries place a greater importance on geometric complexities. Although these segmentation boundaries are identified differently they often correlate (eg. Wasatch fault) and we have found a direct correlation between our newly defined structural boundary and microseismic patterns. This suggests that the Pumpkin Crossing block structural boundary is probably also a seismic segmentation boundary. Although we suggest a seismic segmentation boundary exists we make no predictions about the possibility of a large magnitude earthquake propagating through the study area. The style of deformation observed in this study could potentially serves as a "seismic sink" and absorb great amounts of energy across the numerous faults and folds. This style of deformation may also serve as a "seismic link" where the multiple faults produce many paths for rupture energy and perhaps making it easier for a large magnitude earthquake to propagate through the area.

5. Conclusion

The Clark fault continues past the Santa Rosa segment into the Arroyo Salada segment and ultimately into a newly defined San Felipe Hills segment. The Arroyo Salada segment is ~11-12 km long from multiple branch points west of Smoke Tree Canyon southeast to the Pumpkin Crossing block. It is bounded on the north by the sinistral-normal Truckhaven fault (Janecke, and Axen unpublished mapping) and on the southwest by the dextral San Felipe Hills fault. The San Felipe Hills segment is ~12-13 km long from Pumpkin Crossing block in the northwest to the Extra fault zone in the

southeast. The change observed in microseismicity patterns across the Arroyo Salada and San Felipe Hills segment boundary supports our structural interpretations about the existence, location, and structure of this boundary.

The Clark fault has near 14.5-18 km of right separation in the Santa Rosa segment. Much of the strain is probably represented in the surface deformation of the Arroyo Salada and San Felipe Hills segments but the wide diffuse fault zone with complex deformation patterns and many bedding-strike parallel faults masks the strain. Surface strain from the Clark fault is distributed on about a dozen major structural domains across the Arroyo Salada segment and the northwest part of the San Felipe Hills segment. Each domain contains folds and faults with 1-2 dominant orientations and kinematics. Many faults and some folds are consistent with a wrench fault model but there are many exceptions. Unusual structures are northwest- and northeast-trending folds and the numerous faults with anomalous orientations. We document the interaction between crossing dextral and sinistral faults as interference structures. Such fault arrays interpenetrate, are both currently active, and displace fault domains of the Arroyo Salada and San Felipe Hills segments as well as individual faults through the study area.

Microseismicity combined with fault scarps with dominant southwest-side-down component of slip persist along the central Clark fault traces and show that the Arroyo Salada segment is currently active. A cloud of microseismicity underlies the south end of north-south striking scarps associated with normal east-side-down faults near Salton City. Shadow zones in microseismicity along the Cark fault suggest that the Graves Wash, San Felipe Hills fault and their surrounding areas are either locked or currently inactive. The microseismic alignments dip dominantly northeast whereas the surface deformation along

the central Clark fault zone is dominated by southwest-dipping faults. This requires curved fault surfaces at shallow to mid crustal levels.

References

Anderson, E. M., 1951. The Dynamics of Faulting and Dyke Formation with Applications to Britain, 2nd edition. Oliver and Boyd, Edinburgh.

Allen, C. R., Grantz, A., Brune, J. N., Clark, M. M., Sharp, R. V., Theodore, T. G., Wolfe, E. W., Wyss, M., 1968. The Borrego Mountain, California, earthquake of 9 April 1968 preliminary report. Bulletin of Seismological Society of America 58, 1183-1186.

Bartholomew, M. J., 1968. Geology of the Southern Portion of the fonts point quadrangle and the southwestern portion of the seventeen palms quadrangle, San Diego County, California. M. S. Thesis, University of Southern California.

Bartholomew, M. J., 1970. San Jacinto fault zone in the Imperial Valley, California. Geological Society of America Bulletin 81, 3161-3166.

Belgarde, E. B., Janecke, S., 2006. Structural Characterization and Microseismicity near the SE end of the Clark fault of the San Jacinto fault zone in the SW Salton Trough. Southern California. Abstract for the Annual meeting. Southern California Earthquake Center (SCEC).

Clark, M. M., 1972. Surface rupture along the Coyote Creek Fault. In: Sharp, R.V. (Ed.), The Borrego Mountain earthquake of April 9, 1968; U.S. Geological Survey Professional Paper 787: Reston, VA, United States, 55-86.

Dibblee, T. W., 1954. Geology of the Imperial Valley region, California. In: Jahns, R. H. (Ed.), Geology of southern California, California Division of Mines Bulletin 170, 21-28.

Dibblee, T. W., 1984. Stratigraphy and tectonics of the San Felipe Hills, Borrego Badlands, Superstition Hills and vicinity, In: Rigsby, C. A., (Eds.), The Imperial Basin; tectonics, sedimentation and thermal aspects 40, Pacific Section SEPM Field Trip Guidebook, 31-44.

Dibblee, T. W., 1997. Geology of the Southeastern San Andreas fault zone in the Coachella Velley area, Southern California. In: Baldwin, J., Lewis, L., Payne, M., Roquemore, G., (Eds.), Southern San Andreas Fault – White water to Bombay Beach, Salton Trough, California. South Coast Geological Society Field trip Guidebook 24.

Dorsey, R. J., 2002. Stratigraphic record of Pleistocene initiation and slip on the Coyote Creek fault, lower Coyote Creek, southern California. In: Barth, A. (Ed.), Tectonic evolution southern and Baja California, Sonora and Environs, Geological Society of America, Special Paper 365, 251-269.

Dronyk, M. P., 1977. Stratigarphy, structure and seismic refraction survey of a portion of the San Felipe Hills Imperial Valley, Calfironia, M.S. thesis, University of California.

Eckis, R., 1930. Geology of the southern part of the Indio quadrangle, California. M. S. thesis, California Instituted of Technology.

Feragen, E. S., 1986. Geology of the southeastern San Felipe Hills, Imperial Valley, California. M. S. thesis, San Diego State University.

Fialko, Y. 2006. Interseismic strain accumulation and the earthquake potential on the southern San Andreas fault system. Nature 441, 7096, 968-971.

Fitch, T.J., 1972. Plate convergence, transcurrent faulting and internal deformation adjacent to Southeast Asia and Western Pacific, Journal of Geophysical Research, 77, 4432-4460.

Hauksson, E., 2000. Crustal structure and seismicity distribution adjacent to the Pacific and North America plate boundary in southern California Journal of Geophysical Research 105, 13,875-13,903.

Hauksson, E., Chi, P., Shearer, P., 2004. Comprehensive waveform cross-correlation of southern Califronia seismograms: Part 1. Refined hypocenters obtained using the double-difference method and tectonic implications (abstract), Fall Annual Meeting, American Geophysical Unioun.

Hauksson, E., Shearer, P., 2005. Southern California hypocenter relocation with waveform cross-correlation, Part 1: Results using the double-difference method. Bulletin of the Seismological Society of America 95, 3, 896-902.

Heitman, E. A., 2002. Characteristics of the structural fabric developed at the termination of a major wrench fault. M.S. thesis, San Diego State University, San Diego.

Hill, R. I., 1984. Petrology and Petrogenesis of batholithic rocks, San Jacinto Mountains, southern California. PhD thesis, California Institute of Technology.

Hoover, R.A., 1965. Areal geology and physical stratigraphy of a portion of the southern Santa Rosa Mountains, San Diego County, Califronia. M.A. thesis, University of California.

Hudnut, K., Seeber, L., Rockwell, T.K., Goodmacher, J., Klinger, R., Lindvall, S., McElwain, R., 1989. Surface ruptures on cross-faults in the 24 November 1987 Superstition Hills, California, earthquake sequence: Bulletin of the Seismological Society of America 79, 2, 282-296.

Janecke, S. U., Kirby, S. M., Langenheim, V. E., Steely, A. N., Dorsey, R. J., Housen, B., Lutz, A., 2005. High geologic slip rates on the San Jacinto fault zone in the SW Salton Trough, and possible near-surface slip deficit in sedimentary basins: Geological Society of America Abstracts with Programs 37, no. 7, 275. http://gsa.confex.com/gsa/2005AM/finalprogram/abstract_91941.htm.

Janecke, S. U., S. Kirby, A. Steely, A. Lutz, R. Dorsey, B. Housen, V. Langenheim, 2006. Early Pleistocene emergence of new dextral faults SW of the southern San Andreas fault, Salton Trough: Abstracts for NSF MARGINS program, Workshop on Rupturing of Continental Lithosphere. Ensenada Mexico 46. http://rcl-cortez.wustl.edu/Workshop_Abstracts.pdf.

Jennings, C. W., 1977. Geologic Map of California: California Division of Mines and Geology Geologic Data Map no. 2, scale 1:750,000.

Kennedy, M. P., Morton, D.M., 2003. Preliminary geologic map of the Murrieta 7.5' guadrangle, Riverside County, California. Open-File Report – U.S. Geological Survey 03-417b.

Kirby, S. M., 2005. The Quaternary Tectonic and structural evolution of the San Felipe Hills, California. M.S. thesis, Utah State University.

Kirby, S. M., Janecke, S. U., Dorsey, R. J., Housen, B. A., Langenheim, V. E., McDougall, K. A., Steely, A. N., 2007. Pleistocene Brawley and Ocotillo Formations: Evidence for Initial Strike-Slip Deformation along the San Felipe and San Jacinto Fault Zones Southern California. Journal of Geology 115, 43-62.

Lilly, D. R., 2003. Structural geology of a transitory left step in San Felipe Hills fault. M.S. thesis, San Diego State University.

Lutz, A.T., 2005. Tectonic controls on Pleistocene basin evolution in the central San Jacinto fault zone, southern California. M.S. thesis, University of Oregon.

Lutz A. T., Dorsey, R.J., Housen, B. A., Janecke, S. U., 2006. Stratigraphic record of Pleistocene faulting and basin evolution in the Borrego Badlands, San Jacinto fault zone, southern California. Geological Society of America Bulletin 118, 1377-1397.

Magistrale, H., 2002. The relation of the southern San Jacinto fault zone of the Imperial and Cerro Prieto faults. In: Barth, A., (Ed.) Contributions to Crustal Evolution of the Southwestern United States: Boluder, Colorado, Geological Society of America Special Paper 365, 271-278.

Matti, J. C., Morton, D. M., Cox, B. F., 1985. Distribution and geologic relations of fault systems in the vicinity of the Central Transverse Ranges, southern California. Open-File Report – U.S. Geological Survey 85-365, 23.

Matti, J.C., Morton D.M. 1993. Paleogeographic evolution of the San Andreas Fault in Southern California: A reconstruction based on a new cross-fault correlation. In: Powell, R. E., Weldon, R. J., Matti, J. C. (Eds.), The San Andreas Fault System: Displacement, Palinspastic Reconstruction, and Geologic Evolution. Geological Society of America Memoir 178, 107-159.

Morley, E. R., 1963. Geology of the Borrego Mountain quadrangle and the western portion of the Shell Reef quadrangle, Sand Diego County, California. M. S. thesis, University of Southern California

Morton, D. M., Matti, J. C., 1993. Extension and Contraction within an Evolving Divergent Strike-Slip Fault Complex: The San Andreas and San Jacinto Fault Zones at Their Convergence in Southern California. In: Powell, R. E., Weldon, R. J., Matti, J. C. (eds.), The San Andreas Fault System: Displacement, Palinspastic Reconstruction, and Geologic Evolution: Geological Society of America, Memoir 178, 217-230.

Pettinga, J.R., 1991. Structural styles and basin margin evolution adjacent to the San Jacinto fault zone, Southern California. Geological Society of America, Abstracts with Programs 23, 257.

Richards-Dinger, K.B., Shearer, P.M., 2000. Earthquake locations in southern California obtained using source-specific station terms. Journal of Geophysical Research 105, 10,939-10,960. http://www.data.scec.org/ftp/catalogs/dinger-shearer/

Reitz, D. T., 1977. Geology of the western and central San Felipe Hills, northwestern Imperial County, Califronia. M. S. thesis, University of Southern California

Rogers, T. H., 1965. Santa Ana sheet: California Division of Mines and Geology Geologic Map of Califonria scale, 1:250,000.

Ryter, D.W., 2002. Late Pleistocene kinematics of the central San Jacinto fault zone, southern California. Ph.D. dissertation, University of Oregon.

Sanders, C.O., 1989. Fault segmentation and earthquake occurrence in the strike-slip San Jacinto fault zone, California. In: Schwartz, D.P., Sibson, R.H., (Eds.), Proceedings of Conference XLV; a Workshop on Fault Segmentation and Controls of Rupture Initiation and Termination. Open-File Report – U.S. Geological Survey, 324-349.

Sanders, C., Magistrale, H., 1997. Segmentation of the northern San Jacinto fault zone, Southern California. Journal of Geophysical Research 102, 27453–27467.

Savage, J. C., Prescott, W.H. Lisowski, M., King, N., 1979. Deformation across the Salton Trough, California, Journal of Geophysical Research. 84, B6, 3069-3079.

Sharp, R. V., 1965. Geology of the San Jacinto fault zone in the Peninsular Ranges of southern Califronia. Ph.D. thesis, California Institute of Technology.

Sharp, R. V., 1967. San Jacinto fault zone in the Peninsular Ranges of Southern California. Geological Society of America Bulletin 78, 705-729.

Sharp, R. V., 1972. Map showing recently active breaks along the San Jacinto fault zone between the San Bernardino area and the Borrego Valley, California. U. S. Geological Survey Miscellaneous Geologic Investigations Map I-0675, scale 1:24,000.

Sharp, R. V., 1975. En echelon fault patterns of the San Jacinto Fault zone.: Special Report - California Division of Mines and Geology, no.118, San Andreas Fault in

southern California; a guide to San Andreas Fault from Mexico to Carrizo Plain, 147-152.

Shearer, P., 2002. Parallel fault strands at 9-km depth resolved on the Imperial fault, Southern Califronia. Geophysical Research Letters 29, 14, 19-1 to 19-4.

Shearer, P., Hauksson, E., Lin, G., 2005. Southern California hypocenter relocation with waveform cross-correlation, Part 2: Results using source-specific station terms and cluster analysis. Bulletin of the Seismological Society of America 95, 904-915, http://www.data.scec.org/ftp/catalogs/SHLK/.

Steely, A., 2006. The Evolution from Pliocene West Salton detachment faulting to cross-cutting Pleistocene oblique strike-slip faults in the SW Salton Trough, Southern California. M.S. thesis, Utah State University.

Steely, A., N., Janecke, S. U., Dorsey, R. J., Axen, G. J., submitted 2007. Early Pleistocene initiation of the San Felipe fault zone, SW Salton Trough, during reorganization of the San Andreas fault. Geological Society of America Bulletin.

Suppe J., 2003. Mapping Active Faults in Southern California in 3D Using Small Earthquakes: Southern San Andreas, San Jacinto, and Elsinore Fault Systems. Award # 03HQGR0071.

Thatcher, W., Hileman, J. A., Hanks, T. C., 1975. Seismic slip distribution along the San Jacinto fault zone, southern California and its implications. Geological Society of America Bulletin 86, 1140 –1146.

Thomas, A. P., Rockwell, T. K., 1996. A 300- to 550-year history of slip on the Imperial fault near the U.S.-Mexico border: Missing slip at the Imperial fault bottleneck. Journal of Geophysical Research 101, no. B3, 5987-5998.

Townend, J., Zoback, M. D., 2004. Regional tectonic stress near the San Andreas fault in central and southern California. Geophysical Research Letters 31, LI5S11.

Van Der Pluijm B. A., Marshak, S., 2004. Earth Structure, 2nd edition. W. W. Norton and Company, Incorporated, New York.

Weismeyer, A.L., 1968. Geology of the northern portions of the Seventeen Palms and Fonts Point quadrangles, Imperial and San Diego Counties, California. M. A. thesis, University of Southern California.

Wells, D.L., 1987. Geology of the eastern San Felipe Hills, Imperial Valley, California: implication for wrench fault in the southern San Jacinto Fault zone. M.S. thesis, San Diego State University.

Wesnousky, S.G., 1988. Seismological and structural evolution of strike-slip faults. Nature 335, 340–343.

Wesnousky, S.G., 1989. Seismicity and the Structural Evolution of Strike-Slip Fault Zones, Proceedings of Conference, Fault Segmentation and Controls of Rupture Initiation and Termination, Open-File Report – U.S. Geological Survey 89-315, 193-228.

Wilcox, R.E. Harding, T. P., Seely, D.R., 1973. Basic wrench tectonics. In: Sylvester A. G. (Ed.), Wrench fault tectonics. American Association of Petroleum Geologists.

Withjack, M.O., Jamison, W. R., 1986. Deformation produced by oblique rifting. Tectonophysics 126, 99-124.